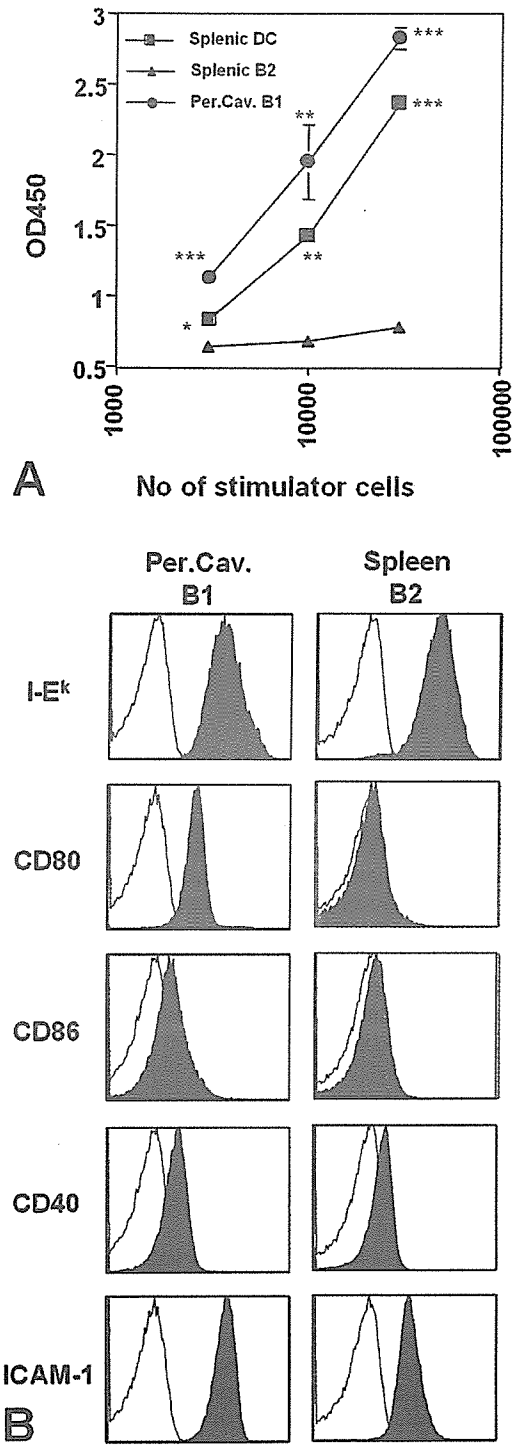

Figure 4. B1 cells as potent APCs. A. Allogeneic mixed lymphocyte reaction (MLR). 3 x 10^5 splenic $CD4^+$ T cells from C57BL/6 mice were co-cultured with either one of mitomycin C treated peritoneal B1 cells, splenic B2 cells or splenic DCs isolated from 2 month-old BWF1 mice. T cell proliferation was assessed by WST-1 assay 96 hr after culture. *p<0.05, **p<0.01, ***p<0.001 as compared to splenic B2 cells. B.Expression of co-stimulatory molecules on B1 and B2 cells. Whole peritoneal cells or splenocytes were stained with B220, CD5 and either one of MHC class II, CD80, CD86, CD40 and ICAM-1. Expression levels of each molecule on gated peritoneal B1 ($CD5^+B220^{lo}$) and splenic B2 ($CD5^-B220^{hi}$) cells are shown (gray histograms). Background staining is also represented as white histograms.

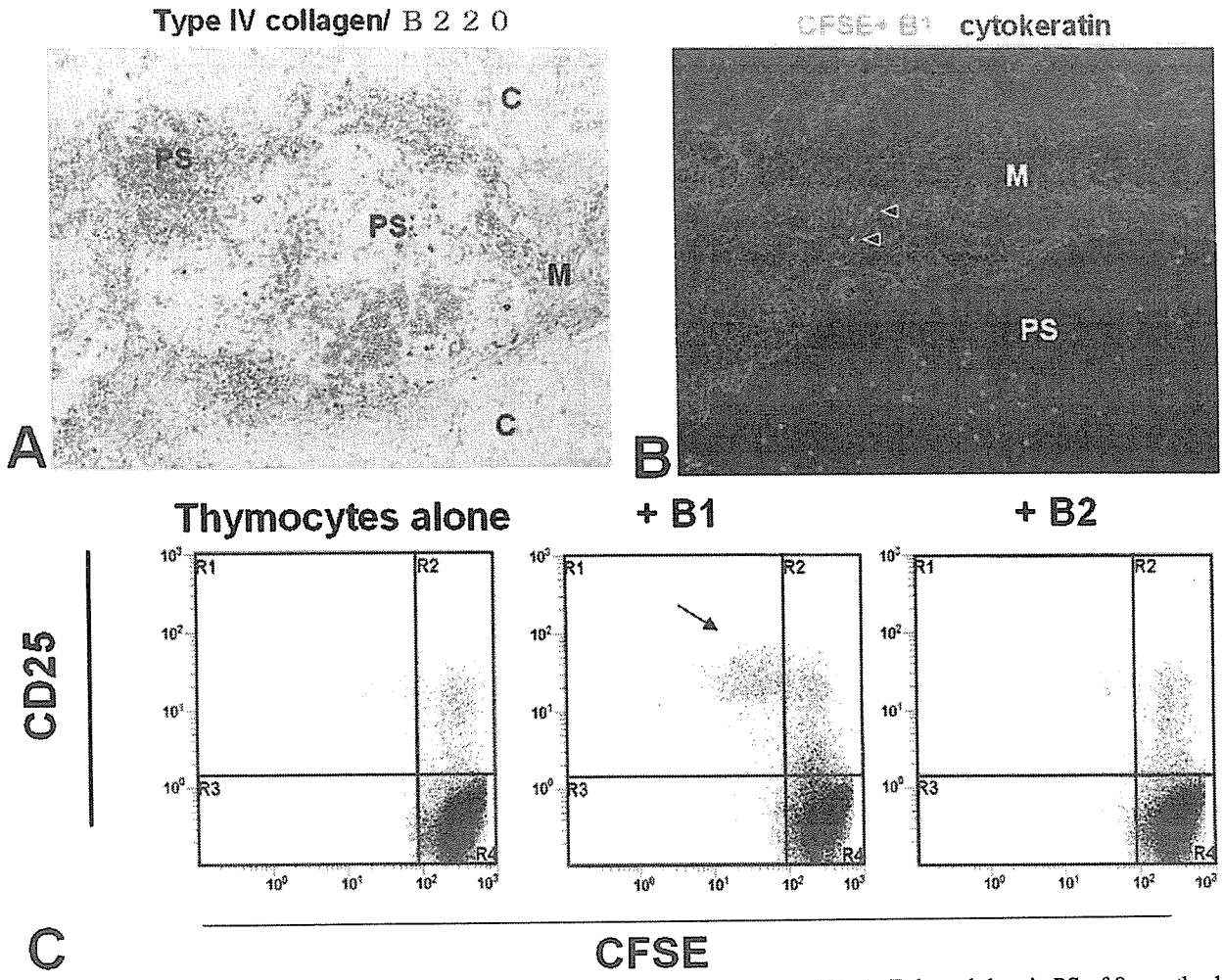

Figure 5. B1 cell migration to enlarged thymic perivascular spaces (PS) in aged BWF1. A. Enlarged thymic PS of 8 month-old BWF1 mice. Frozen sections of thymus from 8 month-old BWF1 mice were doubly stained with antibodies to B220 (red) and either one of cytokeratin (blue) (x200). M:medulla, C:cortex. B. Recruitment of B1 cells into thymic PS and the medulla. Ten million of CFSE-labeled peritoneal B1 cells were transferred intravenously into aged BWF1 mice. Three days later, thymic sections were stained with antibodies to cytokerarin (red) (x200). (C) Activation of self-reactive T cells in the adult thymus by B1 cells. Half million CFSE-labeled adult thymocytes were cultured with 5 x 10^4 of either peritoneal B1 cells or splenic B2 cells in the presence of 5 U/ml of recombinant human IL-2. After 96 hr after culture, cells were stained with FITC anti-CD4 and PE anti-CD25 mAb and analyzed on FCM. Dividing cells are indicated by arrows (gated for CD4 T cells).

but significant number of $CD4^+$ T cells in adult thymus were activated by syngeneic B1, but not B2 cells as evidenced by diluted intensity of CFSE and by CD25 expression (Figure 5C). B1 cells obtained from NZB, NZW, BALB/c and C57BL/6 mice also stimulated proliferation and activation of syngeneic T cells, demonstrating a generalized ability of B1 cells to activate CD4 T cells, some of them being potentially autoreactive. Activated $CD4^+$ T cells showed no TCR Vβ skewing after B1 cell stimulation (unpublished data). Furthermore, B1 cells obtained from MHC class II deficient mice failed to activate thymic CD4 T cells (unpublished data). These data suggest that CD4 T cells were not activated by retroviral superantigens encoded by MMTV, but by self-peptides associated with MHC class II molecules on B1 cells. Possible roles of B1 cell-activated CD4 T cells in the pathogenesis of lupus in BWF1 mice remain to be elucidated.

8. $CXCR5^+CD4$ T CELLS WITH SIMILAR PHENOTYPE TO FOLLICULAR HELPER T CELLS (T_{FH}) MAY BE INVOLVED IN IGG AUTOANTIBODY PRODUCTION BY B1 CELLS IN BWF1 MICE

Recent studies have revealed the existence of the third cellular subset of helper T cells designated as follicular helper T cells (T_{FH}) (29, 30). T_{FH} cells show distinct cytokine profiles from those of Th1 or Th2 cells, and they are able to enhance IgG and IgA antibody production by tonsillar B cells in the absence of APCs. It was also demonstrated that T_{FH} cells express CXCR5, ICOS, CD69 and MHC class II molecules and migrated

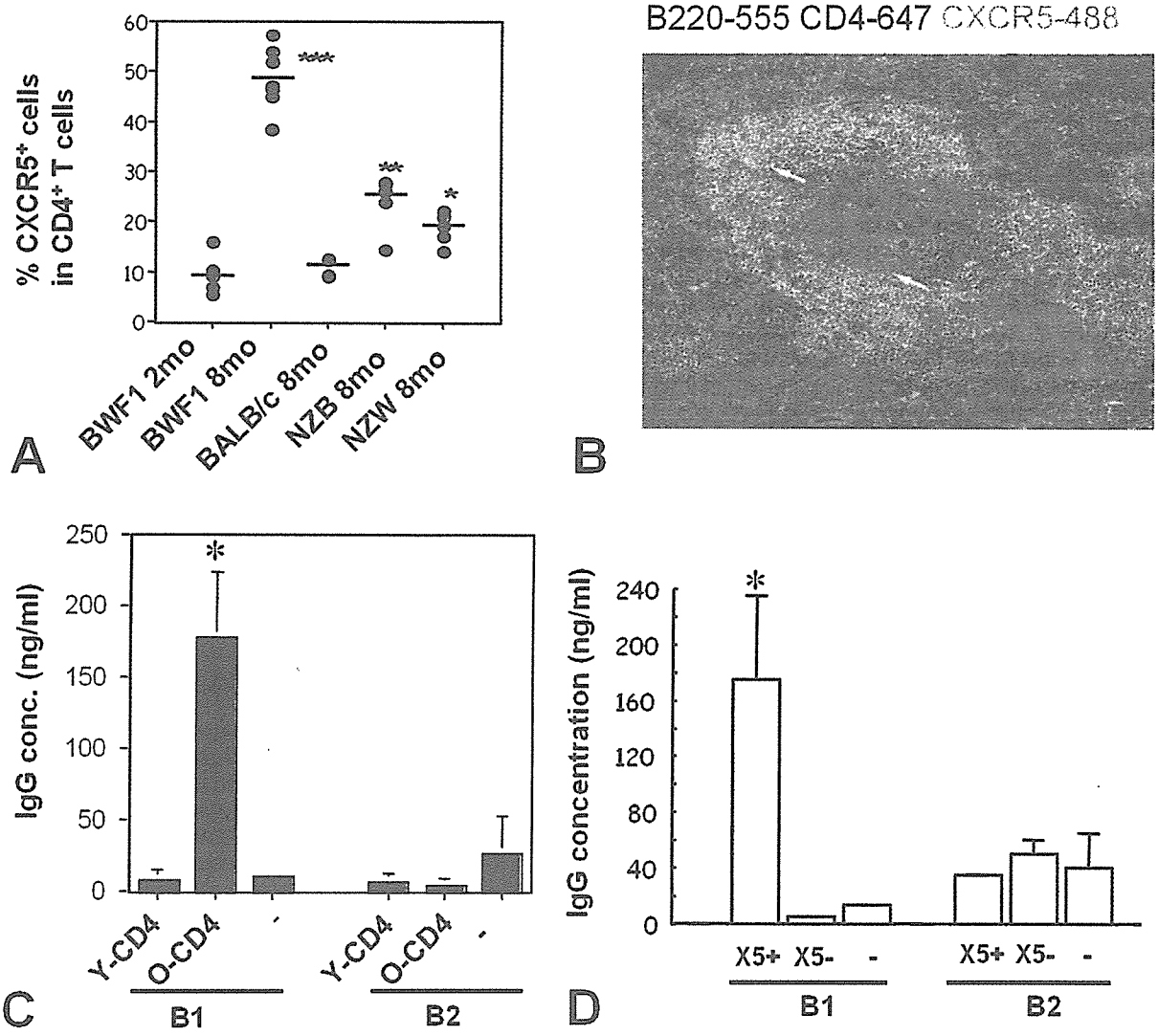

Figure 6. CXCR5$^+$CD4 T cells enhance IgG Ab production by B1 cells. A. Increased frequency of CXCR5$^+$ CD4 T cells in aged BWF1 mice. Spleen cells from young BWF1, aged BWF1, NZB, NZW, BALB/c mice were stained with FITC-anti-CD4 and PE-anti-CXCR5 mAb and analyzed on EPICS flow cytometer. The mean percentage of CXCR5$^+$ CD4 T cells among CD4 T cells were presented. *p<0.02, **p<0.004, *** p<0.000003 as compared to the 2 mo old value. B. Cryostat section of spleen obtained 8 mo-old BWF1 mice stained with Alexa488 labeled-anti-CXCR5 (green), Alexa555 labeled-anti-B220 (red), and Alexa647 labeled-anti-CD4 mAbs and were observed under confocal laser microscopy (x200). CXCR5+ CD4 T cells were localized in T cell area and B cell follicles as indicated by arrows. C. Enhanced IgG antibody production by B1 cells in the presence of CD4 T cells obtained from aged BWF1 mice. CD4 splenic T cells from young or aged BWF1 mice were purified by using anti-CD4 mAb conjugated-MACS beads. Each CD4 T cell population was cultured with peritoneal B (B1 enriched) or splenic B (B2 enriched) cells purified with anti-B220 conjugated-MACS beads. Ten days later, culture supernatants were collected and IgG concentrations were determined by ELISA. * p<0.004 as compared to the group without T cells. D. Enhanced IgG antibody production by B1 cells in the presence of CXCR5$^+$ CD4 T cells. Spleen cells were stained with FITC-anti-CD4 and PE-anti-CXCR5 mAbs and CXCR5$^+$ and CXCR5$^-$ CD4 T cells were sorted on EPICS flow cytometer. Each T cell population was cultured with peritoneal B (B1 enriched) or splenic B (B2 enriched) cells. Ten days later, culture supernatants were collected and IgG concentration was determined by ELISA. * p<0.05.

towards BLC/CXCL13. It has not been examined, however, whether or not T_{FH} cells promote IgG autoantibody production by B1 cells. In aged BWF1 mice, the percentage of CXCR5$^+$ CD4 T cells were markedly increased while similarly aged NZB and NZW mice also showed a much lower percentage of CXCR5$^+$ CD4 T cells (Figure 6A). CXCR5$^+$CD4 T cells in aged BWF1 mice expressed CD69, ICOS, and MHC class II molecules showing a similar cell

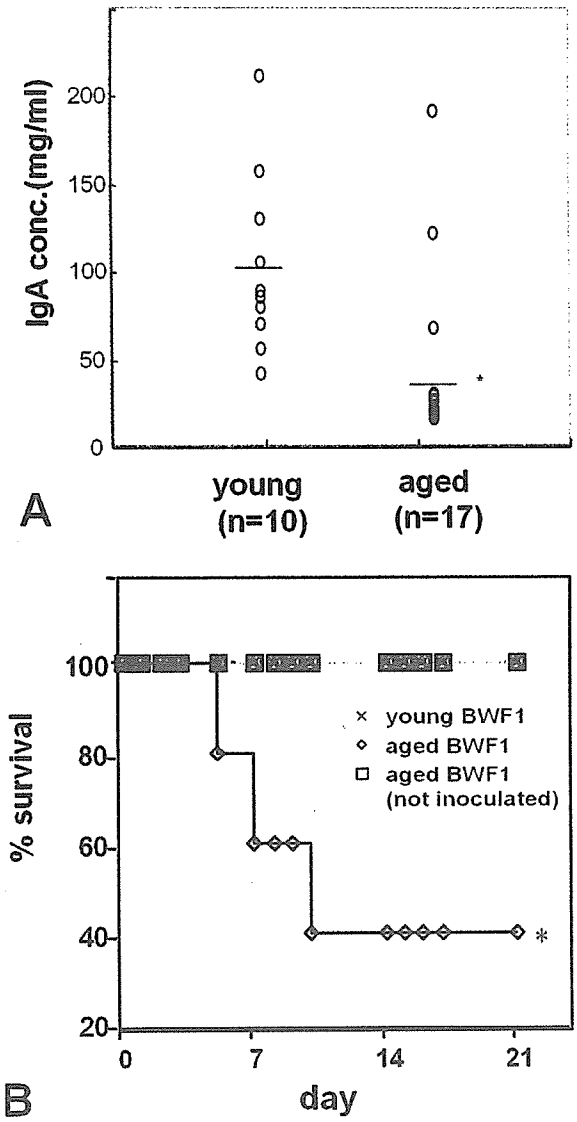

Figure 7. Impaired mucosal immunity in the gut of aged BWF1 mice. A. IgA concentrations in the feces of young and aged BWF1 mice (n=10 and 17, respectively) were determined by ELISA. Each circle represents the IgA level of an individual mouse and bars represent median values. * , P 0.03. B. Increased susceptibility to bacterial infection in aged BWF1 mice. Mice were infected with *E. coli* (10^9 CFU B41 strain) on day 1, 2, 3 and mortality was monitored daily. Each group consisted of five mice: × young BWF1; aged BWF1 infected with *E. coli*; □ aged BWF1 without infection. *p 0.05.

surface phenotype to human tonsillar T_{FH} cells. $CXCR5^+CD4$ T cells were localized in the B cell follicle as well as in the T cell area in the spleen (Figure 6B). CD4 T cells obtained from aged, but not young BWF1 mice enhanced IgG antibody production by B1 cells while they did not enhance IgM production while they had no effect on IgG production by B2 cells from young BWF1 mice (Figure 6C). Anti-ssDNA Ab activity was also detected in the culture supernatants when B1 cells were cultured with CD4 T cells from aged BWF1 mice (data not shown). Furthermore, IgG antibody production by B1 cells was enhanced when B1 cells were cultured with $CXCR5^+$, but not $CXCR5^-$ CD4 T cells (Figure 6D).

9. IMPAIRED MUCOSAL IMMUNITY IN THE GUT IN AGED BWF1 MICE

Kroese *et al.* (31, 32) reported that approximately half of IgA^+ cells in the intestinal lamina propria were derived from B1 cells. It is, therefore, expected that aberrant B1 cell trafficking during the development of lupus in BWF1 mice would result in decreased IgA secretion in the gut. In fact, the level of fecal IgA was dramatically decreased in aged BWF1 mice developing lupus nephritis (Figure 7A) (33). IgA levels in similarly aged NZB and NZW mice remained unchanged (33). All cellular components including CD4 and CD8 T cells, and B cells in Peyer's patches (PPs) were markedly decreased in aged BWF1 mice. Furthermore, aged BWF1 mice showed increased susceptibility to pathogenic bacterial infection (Figure 7B). It was further demonstrated that induction of oral tolerance was impaired and orally administered-antigen induced systemic allergic T cell sensitization in aged BWF1 mice (33).

10. DISCUSSION

Our findings in serial studies suggest that aberrant high expression of BLC/CXCL13 in aged BWF1 mice result in abnormal B1 cell trafficking, activation of self-reactive CD4 T cells and production of IgG autoantibody in the presence of $CXCR5^+CD4$ T cells during the development of murine lupus. Thus, cell trafficking and localization as well as function itself can be an important factor to understand the pathological significance of B1 cells in murine lupus.

Datta and his colleagues (34) previously reported the presence of nucleosome-specific T cells in lupus-prone mice including BWF1 mice, and their helper activity on anti-DNA and histone IgG antibody production. It has been recently reported that nucleosome specific T cells engineered by TCR gene transfer were activated by splenic DCs in BWF1 mice and that the antigen specific regulatory T cells engineered to express CTLA-4 delayed the onset of lupus nephritis (35). On the other hand, autoreactive B1 cells specific for the ribonuclear protein Sm are tolerant or ignorant in the peritoneal cavity (36, 37). Honjo and his colleagues (38) also demonstrated that anti-SRBC B1 cells escape from deletion in the peritoneal cavity in anti-SRBC Ig transgenic mice. These results suggest that the peritoneal cavity is a privileged site for autoreactive B cells to escape from immunological tolerance. Where else it could occur? Interestingly, the same group further demonstrated that anti-SRBC B1 cells did survive in the lamina propria in the gut of anti-SRBC Ig transgenic mice. It is therefore possible that autoreactive B1 cells migrated to the target organs expressing ectopic BLC/CXCL13 escape from tolerance and that they present autoantigens to self-reactive T cells and then are activated by those T cells to produce

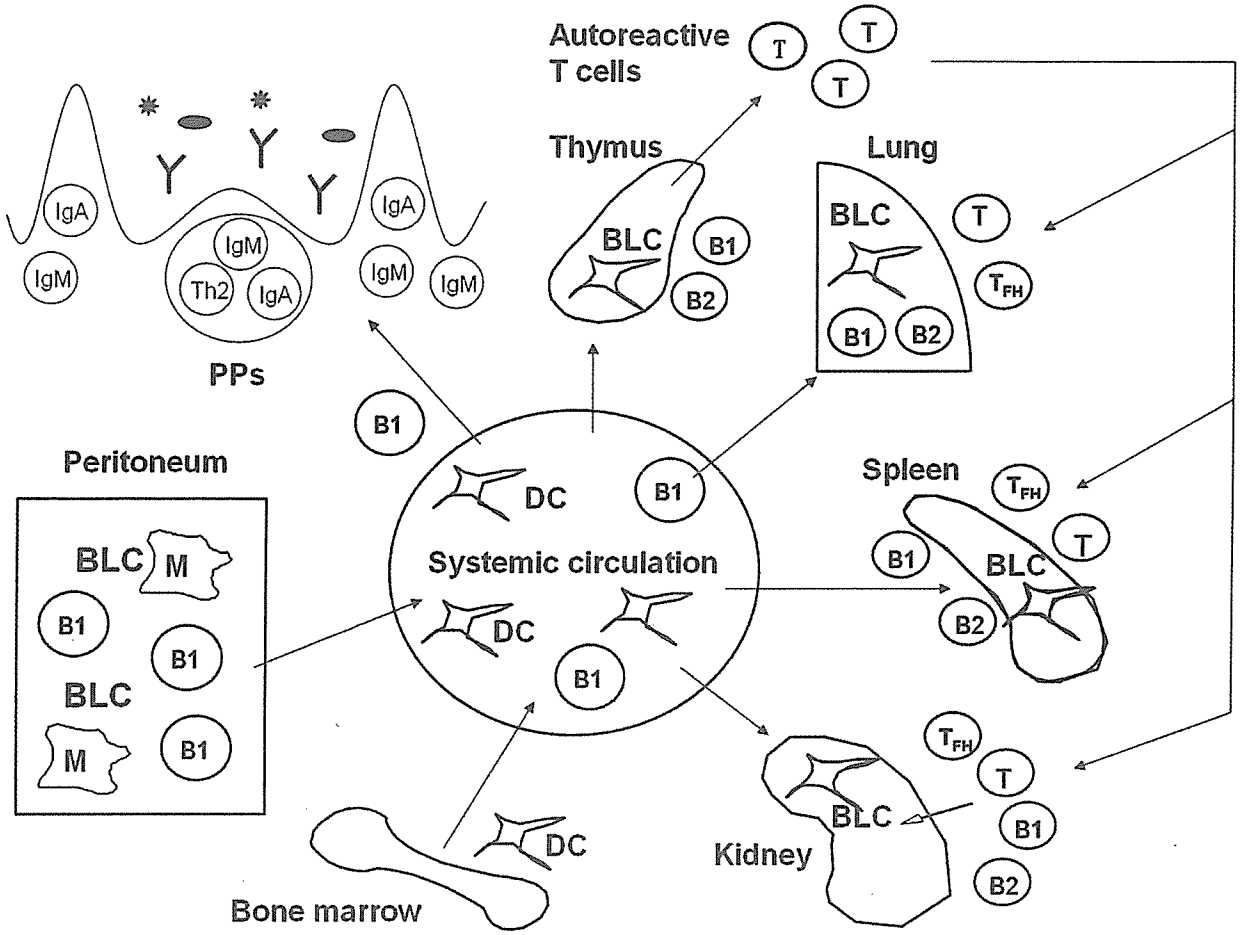

Figure 8. Hypothetical model for pathogenic roles of B1 cells in murine lupus. Aberrant B1 cell trafficking due to ectopic high expression of BLC in aged BWF1 mice results in activation of autoreactive CD4 T cells, IgG autoantibody production in the presence of follicular helper T cells (T_{FH}). DC: dendritic cells, PPs: Peyer's patches, M: macrophages.

autoantibodies. In this context, it is of great interest that B1 cells activate thymic CD4 T cells in the presence of IL-2 although antigenic peptides presented by B1 cells remain to be elucidated. We hypothesize that ectopic high expression of BLC by DCs chemo-attracts B1 and $CXCR5^+$ autoreactive CD4 T cells (T_{FH}-ike?) to form an immunological platform for IgG autoantibody production in the target organs (Figure 8).

Aberrant B1 cell trafficking may also be involved in impaired mucosal immunity in the gut of aged BWF1 mice because B1 cells are the major source of secreted IgA (31,32). IgA production by B1 cells is T cell-independent and requires the presence of commensal microflora (39). Furthermore, commensal bacteria bind mostly B1 cell-derived intestinal IgA, and less so B-2 cell-derived IgA (40). These results favor the idea that immunological stimulation of B1 cells by commensal bacteria at neonatal stage induce IgA production by B1 cells and at the same time develop the mucosal immune system in the gut. Therefore, decreased IgA secretion in aged BWF1 mice may result in penetration of commensal bacteia into systemic immune system. Penetration of commensal bacterial antigen would provoke a vigorous immune response by B1 cells which are specific for polysaccharides such as phosphorylcholine, lipids, and proteins of bacterial components. Unlike mammalian DNA, bacterial DNA has potent immunologic effects that lead to polyclonal B cell activation as well as the production of specific Abs in mice (41). It is also reported that bacterial DNA induces anti-dsDNA antibody cross-reactive to mammalian dsDNA in autoimmune prone mice such as BWF1 mice (42). It is, therefore, tempting to speculate that impaired IgA secretion in the gut lumen and low level of IgM natural antibodies in aged BWF1 mice due to aberrant B1 cell trafficking may result in penetration of commensal bacteria into systemic immune system and induction of vigorous anti-bacterial DNA antibody production which cross-reacts to mammalian DNA. On the other hand, breakdown of oral tolerance in aged BWF1 mice may be attributed to abnormal DC trafficking or antigen trafficking in the intestinal mucosa during the development of lupus.

It is also of interest whether or not stimulation of thymic CD4 T cells by B1 cells in the presence of IL-2 abrogate Treg activity of $CD25^+CD4$ T cells. It is well established that depletion of $CD25^+CD4$ T cells from the thymus or spleen results in autoimmunity in various organs

including the stomach and ovary (43). Although $CD25^+$ CD4 T cells were increased in aged BWF1 mice, their pathological significance in the development of murine lupus remains to be elucidated.

Recent studies have revealed that type-I IFN produced by plasmacytoid DCs (pDCs) play a pivotal role for the pathogenesis of SLE (44, 45). Consistent with findings in SLE patients, it has been also suggested that type-I IFN is involved in the pathogenesis of lupus in BWF1 mice (46, 47). However, the frequency of pDCs in the peripheral blood is very low in aged BWF1 mice (unpublished data), consistent with the study by Farcas *et al.* (48) who demonstrated that pDCs accumulated in the skin in SLE patients while the frequency of pDCs was low in the peripheral blood. It has been also described that pDCs induce plasma cell differentiation through IFN-α and IL-6 (49). A critical role of pDCs for CTL generation has been also documented (50-52). We recently demonstrated a pivotal role of CXCR3/CXCL9 interaction for pDC-transmigration into inflamed LNs through HEVs in bacteria-induced acute hepatitis model (53). Since CXCL9 and CXCL10 expression is also elevated in the target organs in aged BWEF1 mice (unpublished data), it is possible that pDCs migrate to the inflamed target organs and participate in the formation of immunological platform together with B1, T_{FH}, and mDCs.

It still remains unknown what kind of stimuli initiate autoimmune responses in BWF1 mice. Endogenous retroviral activation may be involved in the first step in the development of lupus in BWF1 mice. Lupus-prone mice including BWF1 mice expressed a novel 8.4 kb full-length retroviral transcript corresponding to an endogenous mink cell focus-forming (MCF) env-related provirus (54). Expression of thymic 8.4 kb MCF was detected soon after birth and was determined by bone marrow derived-cells rather than thymic epithelial cells (55,56). Since central tolerance or TCR repertoire formation is completed at the end of gestation, the expression of MCF env-related provirus by bone marrow-derived cells in the thymus just after birth may result in incomplete clonal elimination of MCF virus-specific T cells. It is, therefore, possible that activation of the virus-specific T cells would trigger systemic inflammatory responses including production of inflammatory cytokines/chemokines and generation of apoptotic cells. Plasmacytoid DCs would also produce a large amount of IFN-α at this stage. However, the particular retroviral expression is not enough to induce autoimmune disorders in BWF1 mice because the viral expression is also observed in NZB and NZW mice that do not develop lupus nephritis.

Recent genome-wide searches for susceptibility genes in murine and human SLE have revealed important similarities in the genetic mechanisms mediating SLE in BWF1 mice and humans (57-59). Mohan *et al.* (60) reported that Sle2 on mouse chromosome 4 led to expansion of B1 cells although Sle2 alone on normal B6 background was insufficient to generate anti-nuclear Ab and glomerulonephritis. In consistence with this study, a weak suggestive linkage with syntenic region on human chromosome 9 is reported (61).

Although CD5 molecule is commonly used for discrimination of B1 cells from B2 cells, CD5 may not be the best cell surface marker for B1 cells of human or other species. In human, CD5 is expressed on up to 30 % of B cells in PBL and lymph nodes while in mice, $CD5^+$ B cells are virtually absent from lymph nodes and PBL (18). Although it was demonstrated that human $CD5^+$ B cells selectively expressed a V_H4 subfamily of immunoglobulin genes (62), IgM antibodies bind autoantigens irrespective of CD5 expression (63). In rabbits, all B cells express CD5 molecules (64). These facts may indicate that CD5 expression on B cells in other species does not necessarily mean the same functional B1 subset described in mice. On the other hand, it is reported that unique $RP105^-$ B cells are increased in SLE patients and that the level of these B cells are closely correlated with the disease activity (65). $RP105^-$ B cells lack CD5 expression, but express CD86 and CD38 molecules on their cell surfaces and approximately 50 % of $RP105^-$ B cells express intracytoplasmic IgG although tissue localization, antigen presenting activity, BCR repertoire of $RP105^-$ B cells are not addressed yet. It is, therefore, possible that functional B1 cells with distinct phenotypic characteristics from those in mice are involved in the pathogenesis in human SLE.

11. SUMMARY AND PERSPECTIVE

Aberrant B1 cell trafficking and localization due to ectopic high expression of BLC/CXCL13 may play an important role in the pathogenesis of murine lupus. Pathological significance of $CXCR5^+$ T cells for IgG autoantibody production by B1 cells, of B1 cells for activation of autoreactive CD4 T cells, and of impaired mucosal immunity in the gut for systemic allergic responses in BWF1 mice will be clarified in more details in the near future. Our findings would provide a new insight for pathological significance of B1 cells in the development of SLE and a useful approach to regulate autoimmune responses by targeting B1 cell trafficking.

12. ACKNOWLEDGMENT

This work was supported by SORST (Solution Oriented Research for Science and Technology) by Japan Science and Technology Corporation and LRI (The Long-ranged Research Initiative) by Japan Chemical Industry Association.

13. REFERENCES

1. Hayakawa, K., R.R. Hardy, D.R. Parks & L.A. Herzenberg: The "Ly-1 B" cell subpopulations in normal, immunodefective, and autoimmune mice. *J Exp Med* 157, 202-218 (1983)
2. Hertzenberg, L.A. :The Ly-1 B cell lineage: *Immunol Rev* 93, 81-102. (1986)
3. Hayakawa, K. & R. R. Hardy: Development and function of B-1 cells. *Curr Opin Immunol* 12, 346-353 (2000)

4. Murakami, M., H. Yoshioka, T. Shirai, T. Tsubata, & T. Honjo: Prevention of autoimmune symptoms in autoimmune-prone mice by elimination of B-1 cells. *Int Immunol* 7, 877-882 (1995)
5. Ishida, H., R. Hastings, J. Kearney & M. C. Howard: Continuous anti-interleukin 10 antibody administration depletes mice of Ly-1 B cells but not conventional B cells. *J Exp Med* 175, 1213-1220 (1992)
6. Ishida, H., T. Muchamuel, S. Sakaguchi, S. Andrade, S. Menon, S & M. Howard: Continuous administration of anti-interleukin 10 antibodies delays onset of autoimmunity in NZB/W F1 mice. *J Exp Med* 179, 305-310 (1994)
7. Hayakawa K, R. R. Hardy, M. Honda, L. A. Herzenberg & A. D. Steinberg: Ly-1 B cells: functionally distinct lymphocytes that secrete IgM autoantibodies. *Proc Natl Acad Sci* USA 81, 2494-2498 (1984)
8. Mantovani L, R. L. Wilder & P. Casali: Human rheumatoid B-1a ($CD5^+$ B) cells make somatically hyper-mutated high affinity IgM rheumatoid factors. *J Immunol* 151, 473-489 (1993)
9. Arnold L. W, T. A. Gradina, A. C. Whitmore & G. Haughton: Ig isotype switching in B lymphocytes: isolation and characterization of clonal variants of the murine $Ly\text{-}1^+$ B cell lymphoma, CH12, expressing isotypes other than IgM. *J Immunol* 140, 4355-4363 (1988)
10. Mohan C, L. Morel, P. Yang, & E. K. Wakeland: Accumulation of splenic B1a cells with potent antigen-presenting capability in NZM2410 lupus-prone mice. *Arthritis Rheum* 41, 1652-1662 (1998)
11. Sato T, S. Ishikawa, K. Akadegawa, T. Ito, H. Yurino, M. Kitabatake, H. Yoneyama & K. Matsushima: Aberrant B1 cell migration into the thymus results in activation of CD4 T cells through its potent antigen presenting activity in the development of murine lupus. *Eur J Immunol* 34, 3346-3358 (2004)
12. Lanzavecchia, A.: Antigen-specific interaction between T and B cells. *Nature* 314, 537-539 (1985)
13. Dauphinee, M., Z. Tovar, & N. B. Talal: B cells expressing CD5 are increased in Sjogren's syndrome. *Arthritis Rheum* 31, 642-647 (1998)
14. Plater-Zyberk C., R. N. Maini, K. Lam, T. D. Kennedy, & G. A. Janossy: A rheumatoid arthritis B cell subset expresses a phenotype similar to that in chronic lymphocytic leukemia. *Arthritis Rheum.* 28, 971-976 (1985)
15. Smith H.R. & R. R. Olson: $CD5^+$ B lymphcytes in systemic lupus erythematosus and rheumatoid arthritis. *J Rheumatol* 17, 853-855 (1990)
16. Casali P., S. E. Burastero, J.E. Balow & A. L. Notkins: High affinity antibodies to ssDNA are produced by $CD5^-$ B cells in systemic lupus erythematosus patients. *J Immunol* 143, 3476-3483 (1989)
17. Becker H, C. Weber, S. Storch & K. Federlin: Relationship between $CD5^+$ B lymphocytes and the activity of systemic autoimmunity. *Clin Immunol Immunopathol* 56, 219-225 (1990)
18. Hardy R. R. & K. Hayakawa: Development and physiology of Ly-1 B and its human analog, Leu-1 B. *Immunol Rev* 93. 53-79 (1986)
19. Cong Y. Z., E. Rabin & H. H. Wortis: Treatment of murine $CD5^-$ B cells with anti-Ig, but not LPS, induces surface CD5: two B cell activation pathways. *Int Immunol* 3, 467 476 (1991)
20. Theofilopoulos, A. N.: Murine models of systemic lupus erythematosus. *Adv Immunol.* 37, 269-390 (1985)
21. Shirai T., S. Hirose, T. Okada & H. Nishimura: Immunology and immunopathology of the autoimmune disease of NZB and related mouse strains. In Immunological Disorders in Mice. E. B. Rihova and V. Vetvicka, editors. CRC Press Inc., Boca Raton, p95-136 (1991)
22. Ishikawa S, T. Sato, M. Abe, S. Nagai, N. Onai, H. Yoneyama, Y-Y. Zhang, T. Suzuki, S. Hahismoto, T. Shirai, M. Lipp & K. Matsushima: Aberrant high expression of B lymphocyte chemokine (BLC/CXCL13) in the development of murine lupus and preferential chemotaxis of B1 cells towards BLC. *J Exp Med* 193, 1393-1402 (2001)
23. Forster, R., A.E. Mattis, E. Kremmer, E. Wolf, G. Brem, & M. Lipp: A putative chemokine receptor, BLR1, directs B cell migration to defined lymohoid organs and specific anatomic compartment of the spleen. *Cell* 87, 1037-1047 (1996)
24. Gunn, M.D., V. N. Ngo, K. M. Ansel, E. H. Ekland, J. G. Cyster & L. T. Williams: A B-cell-homing chemokine made in lymphoid follicles activates Burkitt's lymphoma receptor-1. *Nature* 391, 799-803 (1998)
25. Ishikawa S, S, Nagai, T. Sato, K. Akadegawa, H. Yoneyama, Y-Y. Zhang, N. Onai & K. Matsushima: Increased circulating $CD11b^+CD11c^+$ dendritic cells in aged BWF1 mice which can be matured by TNF-□ into BLC/CXCL13 producing-dendritic cells. *Eur J Immunol* 32,1881-1887 (2002)
26. Brennan D. C, M. A. Yui, R. P. Wuthrich & V. E. Kelly: Tumor necrosis factor and IL-1 in New Zealand Black/White mice: Enhanced gene expression and acceleration of renal injury. *J Immunol* 143, 3470 3475 (1989)
27. Ansel KM, R. B. Harris & J. G. Cyster: CXCL13 is required for B1 cell homing, natural antibody production, and body cavity immunity. *Immunity* 16, 67-76 (2002)
28. Ito T, S. Ishikawa, T. Sato, K. Akadegawa, H. Yurino, M. Kitabatake, S. Hontsu, T. Ezaki, H. Kimura & K. Matsushima: Defective B1 cell homing to the peritoneal cavity and preferential recruitment of B1 cells in the target organs in a murine model for SLE. *J Immunol* 172, 3628-3634 (2004)
29. Scharli P, K. Willimann, A. B. Lang, M. Lipp, P. Loetscher & B. Moser: CXC chemokine receptor 5 expression defines follicular homing T cells with B cell helper function. *J Exp Med* 192, 1553-1562 (2000)
30. Breitfeld D, L. Ohl, E. Kremmer, J. Ellwart, F. Sallusto, M. Lipp & R. Forster: Follicular B helper T cells express CXC chemokine receptor 5, localize to B cell follicles, and support immunoglobulin production. *J Exp Med* 192, 1545-1552 (2000)
31. Kroese F. G. M, W. A. Ammerlaan & A. B. Kantor. Many of the IgA producing plasma cells in murine gut are derived from self-replenishing precursors in the peritoneal cavity. *Int Immunol* 1, 75-84 (1989)
32. Kroese F. G. M., W. A. Ammerlaan & A. B. Kantor: Evidence that intestinal IgA plasma cells in transgenic mice

are derived from B-1 (Ly-1 B) cells. *Int Immunol* 5, 1317-1327 (1993)
33. Akadegawa K, S, Ishikawa, T. Sato, J. Suzuki, H. Yurino, M. Kitabatake, T. Ito, T. Kuriyama & K. Matsushima. Breakdown of mucosal immunity in the gut and resultant systemic sensitization by oral antigens in a murine model for SLE. *J Immunol* 174, 5499-5506 (2005)
34. Mohan C., S. Adams, V. Stanik, & S. K. Datta. Nucleosome: A major immunogen for pathogenic autoantibody-inducing T cells of lupus. *J Exp Med* 177, 1367-1381 (1999)
35. Fujio K., A. Okamoto, H. Tahara, M. Abe, Y. Jiang, T. Kitamura, S. Hirose, & K. Yamamoto. Nucleosome-specific regulatory T cells engineered by triple gene transfer suppress a systemic autoimmune disease. *J Immunol* 173, 2118-2125 (2004)
36. Qian Y., H. Wang, & S. H. Clarke. Impaired clearance of apoptotic cells induces the activation of autoreactive anti-Sm marginal zone and B-1 B cells. *J Immunol* 172, 625-635 (2004)
37. Qian Y., C. Santiago, M. Borrero, T. F. Tedder & S. H. Clarke. Lupus-specific anti-ribonucleoprotein B cell tolerance in non-autoimmune mice is maintained by differentiation to B-1 and governed by B cell receptor signaling thresholds. *J Immunol* 166, 2412-2419 (2001)
38. Murakami M., T. Tsubata, R. Shinkura, S. Nishitani, M. Okamoto, H. Yoshioka, T. Usui, S. Miyawaki, & T. Honjo. Oral administration of lipopolysaccharides activates B-1 cells in the peritoneal cavity and lamina propria of the gut and induces autoimmune symptoms in an autoantibody transgenic mouse. *J Exp Med* 180, 111-121 (1994)
39. Macpherson A. J., D. Gatto, E. Sainsbury, G. R. Harriman, H. Hengartner & R. M. Zinkernagel: A primitive T cell-independent mechanism of intestinal mucosal IgA responses to commensal bacteria. *Science* 288, 2222-2226 (2000)
40. Bos N. A., J. C. Bun, S. H. Popma, E. R. Cebra, G. J. Deenen, M. J. van der Cammen, F. G. Kroese & J. J. Cebra: Monoclonal immunoglobulin A derived from peritoneal B cells is encoded by both germline and somatically mutated VH genes and is selective with commensal bacteria. *Infect Immun* 64: 616-623 (1996)
41. Gilkeson, G. S., J. Grudier & D. S. Pisetky: Specificity of anti-DNA antibodies induced in normal mice by immunization with bacterial DNA *Clin Immunol Immunopathol* 59, 288-300 (1991)
42. Gilkeson, G. S., M. M. Pippen, and D. S. Pisetky: Induction of cross-reactive anti-DNA antibodies in preautoimmune NZB/NZW mice by immunization with bacterial DNA. *J Clin Invest* 95, 1398-1402 (1995)
43. Sakaguchi S. Regulatory T cells: key controllers in immunologic self-tolerance. Cell 101, 455-458 (2000)
44. Blanco P. A. K. Palucka, M. Gill, V. Pascual, & J. Banchereau. Induction of dendritic cell differentiation by IFN-alpha in systemic lupus erythematosus. *Science* 294, 1540-1543 (2001)
45. Pascual V., J. Banchereau, & A. K. Palucka. The central role of dendritic cells and interferon-a in SLE. *Curr Opin Immunol* 15, 548-556 (2003)
46. Santiago-Raber M.-L., R. Baccala, K. M. Haraldsson, D. Choubey, T. A. Stewart, D. H. Kono, & A. N. Theophilopoulos. Type-I interferon receptor deficiency reduces lupus-like disease in NZB mice. *J Exp Med* 197, 777-788 (2003)
47. Mathian A., A. Weinberg, M. Gallegos, J. Banchereau, & S. Koutouzov. IFN-a induces early lethal lupus in preautoimmune (New Zealand Black x New Zealand White) F1 but not in BALB/c mice. *J Immunol* 174, 2499-2506 (2005)
48. Farcas L., K. Beiske, F. Lund-Jahnsen, P. Brandtzaeg, & F. L. Jahnsen. Plasmacytoid dendritic cells (natural interferon-α/β-producing cells) accumulate in cutaneous lupus erythematosus lesions. *Am J Pathol* 159, 237-243 (2001)
49. Jego G., A. K. Palucka, J-P. Blanck, C. Chalouni, V. Pascual, & J. Banchereau. *Immunity* 19, 225-234 (2003)
50. Yoneyama H., K. Matsuno, E. Toda, T. Nishiwaki, N. Matsuo, A. Nakano, S. Narumi, B. Lu, C. Gerald, S. Ishikawa, K. Matsushima. Plasmacytoid dendritic cells help lymph node dendritic cells to induce anti-HSV CTLs. *J Exp Med* 202, 425-435 (2005)
51. Allan, R. S., C. M. Smith, G. T. Belz, A. L. von Lint, L. M. Walin, W. R. Heath, & F. R. Carbone. Epidermal viral immunity induced by CD8alpha+ dendritic cells but not Langerhans cells. *Science* 301, 1925-1928 (2003)
52. Krug A., O. Rosorius, F. Kratzer, G. Sterz, C. Cuhnt, G. Schulera, J. Hauber, & M. Cella. Interferon-producing cells fail to induce proliferation of naïve T cells but can promote expansion of antigen-experienced unpolarized T cells. *J Exp Med* 197, 899-906 (2003)
53. Yoneyama H., K. Matsuno, Y-Y. Zhang, T. Nichiwaki, M. Kitabatake, S. Ueha, S. Narumi, S. Morikawa, T. Ezaki, B. Lu, S. Ishikawa, & K. Matsushima. Evidence for recruitment of plasmacytoid dendritic cell precursors to inflamed lymph nodes through high endothelial venules. *Int Immunol.* 16, 915-928 (2004)
54. Krieg, A. M., A. D. Steinberg, A & A. S. Khan: Increased expression of novel full length endogenous mink cell-focus-forming-related transcripts in autoimmune prone mouse strains. *Virology* 162, 274-276 (1988)
55. Krieg A. M., W. C. Gause, M. F. Courley, & A. D. Steinberg: A role for endogenous retroviral sequences in the regulation of lymphocyte activation. *J Immunol* 143, 2448-2451 (1989)
56. Krieg A. M., M. F. Courley, & A. D. Steinberg. Association of murine lupus and thymic full length endogenous retroviral expression maps to a bone marrow stem cell. *J Immunol* 146, 3002-3005 (1991)
57. Morel L., U. H. Rudofsky, J. A. Longmate, K. Schiffenbauer & E. K. Wakeland: Polygenic control of susceptibility to murine systemic lupus erythematosus. *Immunity* 1, 219-229 (1994)
58. Kotzin, B. L. Systemic lupus erythematosus. *Cell* 85, 303-306 (1996)
59. Wakeland E. K., A. E. Wandstrat, K. Liu & L. Morel: Genetic dissection of systemic lupus erythematosus. *Curr Opin Immunol* 11, 701-707 (1999)
60. Mohan C, L. Morel, P. Yang & E. K. Wakeland: Genetic dissection of systemic lupus erythematosus pathogenesis; Sle2 on murine chromosome 4 leads to B cell heperactivity. *J Immunol* 159, 454-465 (1997)
61. Nath S. K., A. I. Quintero-Del-Rio, J. Kilpatrick, L. Feo, M. Ballesteros & J. B. Haley: Linkage at 12q24 with systemic lupus erythematosus (SLE) is established and

confirmed in Hispanic and European American families. *Am J Hum Genet* 74, 73-82 (2004)
62. Mageed R.A., L. MacKenzie, F. K. Stevenson, B. Yuksel, F. Shokri, B. R. Maziak, R. Jefferis & P. M. Lydyard: Selective expression of VHIV subfamily of immunoglobulin genes in human $CD5^+$ B lymphocytes from cord blood. *J Exp Med* 174, 109-113 (1991)
63. Deane M, L. MacKenzie, F. K. Stevenson, P.Youinou, P. M. Lydyard & R. A. Mageed: The genetic basis of human V_H4 gene family-associated cross-reactive idiotype expression in $CD5^+$ and $CD5^-$ cord blood B lymphocyte clones. *Scand J Immunnol* 38, 348-358 (1993)
64. Raman C & K.L. Knight: $CD5^+$ B cells predominate in peripheral tissues of rabbit. *J Immunol* 149, 3858-3864 (1992)
65. Koarada S, Y. Tada, O. Ushiyama, F. Morito, N. Suzuki, A. Ohta, K. Miyake, M. Kimoto & K. Nagasawa: B cells lacking RP105, a novel B cell antigen, in systemic lupus erythematosus. *Arthritis Rhemat* 42, 2593-2600 (1999)

Key Words: Systemic Lupus Erythematosus, SLE, chemokine, B cell, Immune System, Autoantibody, Review

Send correspondence to: Sho Ishikawa, PhD, MD, Associate Professor, Department of Molecular Preventive Medicine, School of Medicine, The University of Tokyo, Tokyo , 7-3-1 Hongo, Bunkyo-ku, Tokyo 113-0033, Japan, Tel: 81-3-5841-3677, Fax: 81-3-5841-3393, E-mail: yamasho@m.u-tokyo.ac.jp

http://www.bioscience.org/current/vol12.htm

Bioconjugate Chem. 2006, *17*, 899–904

Induction of Differential T-Cell Epitope by Plain- and Liposome-Coupled Antigen

Maiko Taneichi,† Yuriko Tanaka,† Michiyuki Kasai,† Masahito Mori,‡ Mitsuhiro Nishida,‡ Hiroyuki Yamamura,‡ Junichiro Mizuguchi,§ and Tetsuya Uchida†,*

Department of Safety Research on Blood and Biological Products, National Institute of Infectious Diseases, Tokyo 208-0011, Japan, Drug Delivery System Development Division, Nippon Oil and Fat Corporation, Tokyo 150-6019, Japan, and Department of Immunology, Tokyo Medical University, Tokyo 160-8402, Japan. Received January 31, 2006; Revised Manuscript Received April 30, 2006

The T-cell receptors of $CD4^+$ T lymphocytes recognize immunogenic peptide sequences bound within the groove of MHC class II molecules, and the peptides that bind to these molecules are known to share common structural motifs. For example, $OVA_{323-339}$, an I-A^d-binding peptide, involves a motif of the I-A^d peptide-binding groove. In the present study, OVA peptides of up to 26-mer were sequentially synthesized and screened, and two additional I-A^d binding OVA peptides, OVA_{20-43} and $OVA_{264-286}$, were found to stimulate $CD4^+$ T cells of OVA-immune BALB/c mice. OVA_{20-43} involved structural motifs of the I-A^d peptide-binding groove, while $OVA_{264-286}$ did not. The ability of these three I-A^d binding OVA peptides to induce antigen-specific cytokine production was compared among $CD4^+$ T cells of mice immunized either with alum-adsorbed OVA (OVA−alum) or OVA chemically coupled to the surface of liposome (OVA−liposome). $CD4^+$ T cells of mice immunized with OVA−alum produced more cytokines when stimulated with $OVA_{264-286}$ than with $OVA_{323-339}$, while $CD4^+$ T cells of mice immunized with OVA−liposome conjugates produced more cytokines when stimulated with $OVA_{323-339}$ than with $OVA_{264-286}$. OVA_{20-43} induced production of comparable levels of cytokines in mice immunized either with OVA−alum or OVA−liposome. Confocal laser scanning microscopic analysis demonstrated that chemically coupled OVA and liposomes were colocalized in APCs until OVA received processing. Three-dimensional structural analysis demonstrated that both $OVA_{264-286}$ and $OVA_{323-339}$ were present on the surface of OVA, but OVA_{20-43} was not. These results suggested that the chemical coupling of OVA to liposome affected antigen processing in APCs and thus resulted in the induction of differential T-cell epitopes as compared with those induced by plain OVA.

INTRODUCTION

In general, T-cell receptors (TCRs) of $CD4^+$ T cells do not recognize native protein antigens, but do recognize antigenic peptides displayed in association with major histocompatibility complex (MHC) class II molecules by antigen-presenting cells (APCs). TCRs occur as either of two distinct heterodimers, $\alpha\beta$ or $\gamma\delta$. The $\alpha\beta$ TCR heterodimer-expressing cells predominate in most lymphoid compartments (90% to 95%) of humans and mice and are responsible for the classical helper or cytotoxic T cell responses. In most cases, the $\alpha\beta$ TCR ligand is a peptide antigen bound to the class I and class II MHC molecule (*1*). Class I and II molecules encoded by genes within the MHC play a central role in regulating immune responses through their ability to bind and display small peptides derived from foreign antigens.

Grey and co-workers identified ovalbumin (OVA) peptide 323−339 as being immunodominant in H-2^d mice (*2*) and showed that this peptide binds to I-A^d, but not I-E^d, the latter of which is an Ia molecule that will not present this peptide (*3*). Ever since $OVA_{323-339}$ was identified, it has been used extensively to study the nature of class II MHC-peptide binding and T-cell activation (*4*−*9*). However, this peptide is responsible for 25−35% of the T-cell responses in BALB/c mice immunized with whole ovalbumin (*2*), suggesting the presence of other I-A^d binding OVA peptides with T-cell stimulatory activity while, at present, no other I-A^d binding OVA peptides have been reported.

We previously reported that OVA chemically coupled to the surface of liposomes via glutaraldehyde (OVA−liposome conjugates) induced IgE-selective unresponsiveness in mice (*10*). The IgE-selective unresponsiveness was induced by antigen−liposome conjugates, regardless of the coupling procedure of antigen and liposomes (*11*), using liposomes of different lipid formulations (*12*), or using different antigens such as tetanus toxin (*13*) or Shiga-like toxin (*14*). Thus, antigen−liposome conjugates are expected to be applicable as part of a novel protocol for the development of vaccines that would induce minimal IgE synthesis.

In the present study, sequentially synthesized OVA peptides were screened for the ability to stimulate OVA-specific $CD4^+$ T cells of BALB/c (H-2^d) mice and two additional I-A^d binding OVA peptides, OVA_{20-43} and $OVA_{264-286}$, were found. The ability of these three OVA peptides to stimulate $CD4^+$ T cells of OVA-immune BALB/c mice was compared among the $CD4^+$ T cells of mice immunized either with OVA−alum or with OVA−liposome conjugates. The aim of this study was to investigate the effect of antigen modification on the in vivo induction of T cell epitopes.

EXPERIMENTAL PROCEDURES

Mice. BALB/c mice (female, 8 weeks of age) were purchased from Charles River, Kanagawa, Japan. The mice were maintained in sterile cages under specific pathogen-free conditions at the Division of Experimental Animals Research (National Institute of Infectious Diseases, Tokyo, Japan).

* To whom correspondence should be addressed. Tel: +81-42-561-0771; Fax: +81-42-562-7892. E-mail: tuchida@nih.go.jp.
† National Institute of Infectious Diseases.
‡ Nippon Oil and Fat Corporation.
§ Tokyo Medical University.

10.1021/bc060024g CCC: $33.50
Published on Web 06/21/2006

Antigens. Ovalbumin (OVA, Grade VII) was purchased from Sigma (St. Louis, MO). For analysis of the processing of liposome-coupled OVA by macrophages, DQ−OVA, which exhibits green fluorescence upon proteolytic degradation, was purchased from Molecular Probes, Inc. (Eugene, OR).

OVA Peptides. OVA peptides consisting of 20−26 amino residues were sequentially synthesized, and the ability of each peptide to induce cytokine production by $CD4^+$ T cells of BALB/c mice immunized with OVA was investigated. All OVA peptides used in the present study were synthesized and supplied by Operon Biotechnologies, K. K. (Tokyo, Japan). Precursor peptide material attached to polystyrene resin was synthesized by an automated peptide synthesizer (model 433A; Applied Biosystems, Foster City, CA) using Fmoc (9-fluorenylmethoxycarbonyl) chemistry. Then, the resins on the peptide C-terminus and the building blocks on the peptide side chain were removed by trifluoroacetic acid. The purification of the peptide was performed by high-performance liquid chromatography (HPLC) using an automated system (HPLC-10A; Shimazu Co., Kyoto, Japan) with a 35−55% acetonitrile gradient in the acidic aqueous phase. As a result, the highly purified material was obtained with a >95% area ratio on the HPLC elution chart and was determined by mass spectroscopic analysis with the matrix-assisted laser desorption/ionization time-of-flight method using Applied Biosystems Voyager DE. The peptide solution was lyophilized and used for the subsequent experiments.

Fluorescence Labeling of OVA. OVA were labeled with fluorescence using an Alexa Fluor 488 protein labeling kit (Molecular Probes, Inc.) following the manufacturer's protocol. The estimated F:P ratio of Alexa Fluor 488−OVA conjugate was 1.4:1.

Chemicals. All phospholipids were obtained from NOF Co., Tokyo, Japan. Reagent grades of cholesterol were purchased from Wako Pure Chemical Industries, Osaka, Japan.

Liposomes. The liposomes used in the present study consisted of dipalmitoyl phosphatidylcholine, dipalmitoyl phosphatidyl ethanolamine, cholesterol, and dimyristoyl phosphatidyl glycerol in 4:3:7:2 molar ratios. The crude liposome solution was passed through a membrane filter (Nucleopore polycarbonate filter, Coster, Cambridge, MA) with a pore size of 0.2 μm.

Red-Labeled liposome. Red-labeled liposomes were prepared by adding 1,2-dimyristoyl-sn-glycero-3-phosphoethanolamine-*N*-(lissamine rhodamine B sulfonyl) (Product Number: 810157, Avanti Polar Lipids Inc, Alabaster, AL) into the above lipid constituent of liposomes.

Coupling of OVA to Liposomes. Liposomal conjugates with plain OVA, Alexa−OVA, or DQ−OVA were prepared essentially in the same way as described previously (*15*) via glutaraldehyde. Briefly, to a mixture of 90 mg of liposomes and 6 mg of OVA in 2.5 mL of phosphate buffer (pH 7.2) was added 0.5 mL drops of 2.5% glutaraldehyde solution. The mixture was stirred gently for 1 h at 37 °C, and then 0.5 mL of 3 M glycine−NaOH (pH 7.2) was added to block excess aldehyde groups. This was followed by incubation overnight at 4 °C. The liposome-coupled OVA and uncoupled OVA in the resulting solution were separated using CL-4B column chromatography (Pharmacia Fine Chemical Co., Upsala, Sweden). The amount of lipid in the liposomal fraction was measured using a Phospholipid-Test-Wako phospholipid content assay kit (Wako Pure Chemical Industries). The OVA−liposome solution was adjusted to 10 mg lipid/mL in RPMI-1640, sterile-filtered using a Millex-HA syringe filter unit (0.45 μm, Millipore Corp., Bedford, MA), and kept at 4 °C until use.

Immunization. The mice were immunized intraperitoneally (ip) with 200 μL of 10 μg of OVA adsorbed with 100 μg of alum (Alhydrogel, Superfos Biosector, Vedbaek, Denmark) in PBS or with 200 μL of OVA−liposome conjugates, at 0 and 4 weeks.

Preparation of Splenic Adherent Cells. Splenic adherent cells (SACs) were used as antigen-presenting cells in the cultures of the $CD4^+$ T cells and OVA peptides. SACs were obtained from naive BALB/c mice as follows. Spleen cell suspensions were prepared in RPMI-1640 containing 10% fetal calf serum (FCS). Cells (5×10^7) in 5 mL of medium containing 10% FCS were plated into 50-mm plastic tissue culture dishes (No. 3002; Becton-Dickinson Labware, Franklin Lakes, NJ) and incubated at 37 °C in a humidified 5% CO_2 atmosphere for 2 h. After culture, nonadherent cells were removed by three vigorous washings in warm media, and adherent cells were then harvested with a cell scraper.

Preparation of $CD4^+$ T Cells. $CD4^+$ T-cell purification from spleen cells of mice immunized with OVA−alum was performed with the MACS magnetic cell sorter system (Miltenyi Biotec GmbH, Bergisch Gladbach, Germany) according to the manufacturer's protocol and using anti-CD4 antibody-coated microbeads (No. 492-01; Miltenyi Biotec). $CD4^+$ T cells were suspended in RPMI-1640 containing 10% FCS at a cell density of 2×10^6/mL. In the present study, OVA peptides at a final concentration of 10 μM with 1 and 5 d culture periods were employed for the production of the Th1 (IL-2, IFN-γ) and Th2 (IL-4, IL-5) cytokines, respectively. The $CD4^+$ T-cell suspension was plated at 250 μL per well onto 48-well culture plates (No. 3047; Becton-Dickinson Labware), and 500 μL of 20 μM OVA peptide solution and 250 μL of 8×10^5/mL SAC in the same medium were added to the plates. After incubation in a CO_2 incubator, the culture supernatants were collected and assayed to determine the concentrations of cytokines.

Cytokine Assays. IL-5 and IFN-γ in the culture supernatant were measured using the Biotrak mouse ELISA system (Amersham International, Buckinghamshire, UK). All test samples were assayed in duplicate, and the standard error in each test was always less than 5% of the mean value.

Cloned Macrophage Hybridoma. Macrophage hybridoma clone No. 39, obtained from the fusion of splenic adherent cells from CKB mice and $P388D_1$ (*16*), was maintained in RPMI-1640 (Gibco Laboratories, Grand Island, NY) supplemented with 10% heat-inactivated FCS (Hyclone Laboratories, Logan, UT), 100 U/mL of penicillin, and 100 μg/mL of streptomycin (Gibco Laboratories) in a 75 cm^2 flask (No. 3111; Becton Dickinson Labware, Franklin Lakes, NJ).

Flow Cytometry. To investigate the processing of OVA coupled to liposome by macrophages, #39 macrophage clone was incubated for 15 to 60 min at 37 °C in the presence of DQ−OVA−liposome conjugates that contained a final concentration of 4 μg/mL OVA. After incubation, the cells were washed with ice-cold PBS and then were analyzed on a FACS Calibur flow cytometer (BD Biosciences, Mountain View, CA). The histograms of fluorescence distribution were plotted as the number of cells versus fluorescence intensity on a logarithmic scale.

Confocal Laser Scanning Microscopy. To investigate the processing of liposome-coupled OVA by macrophages, macrophage clone No. 39 was cultured for 18 h at 37°C on 8-hole heavy Teflon-coated slides (Bokusui Brown, New York, NY) and then incubated with DQ−OVA−liposome conjugates for 2 h at 37 °C. The slides were washed with MEM and fixed with 4% paraformaldehyde in PBS for 10 min at room temperature. After fixation, they were incubated for 10 min in 0.1 M glycine-HCl, pH 7.0, to block the remaining ardehyde residue. They were then washed two times in PBS. After washing, the slides were sealed with PBS/glycerin (PBS:glycerin = 1:9). They were then analyzed under a confocal laser scanning

Table 1. OVA Peptides Investigated in the Present Study

OVA peptides	amino acid sequence
1–20	GSIGAASMEFCFDVFKELKV
20–43	VHHANENIFYCPIAIMSALAMVYL
53–78	INKVVRFDKLPGFGDSIEAQCGTSVN
61–85	KLPGFGDSIEAQCGTSVNVHSSLRD
164–181	SSVDSQTAMVLVNAIVFK
190–207	DEDTQAMPFRVTEQESKP
220–245	ASMASEKMKILELPFASGTMSMLVLL
264–286	LTEWTSSNVMEERKIKVYLPRMK
302–327	ITDVFSSSANLSGISSAESLKISQAV
323–339	ISQAVHAAHAEINEAGR

Table 2. Induction of Cytokine Production by OVA Peptides[a]

OVA peptides	IL-2	IL-4	IL-5	IFN-γ
1–20	ND	ND	ND	ND
20–43	278.3 ± 53.5	221.2 ± 78.1	1201.5 ± 58.3	1275.5 ± 507.9
53–78	ND	ND	ND	ND
61–85	ND	ND	ND	ND
164–181	ND	ND	ND	ND
190–207	ND	ND	ND	ND
220–245	ND	ND	ND	ND
264–286	511.7 ± 85.0	140.3 ± 28.3	1073.4 ± 156.3	1321.6 ± 260.7
302–327	ND	ND	ND	ND
323–339	215.6 ± 35.5	27.8 ± 15.1	560.1 ± 51.1	302.6 ± 72.6
OVA	856.7 ± 60.8	78.0 ± 30.1	1133.4 ± 39.1	2457.0 ± 667.3

[a] Each peptide was assessed for its ability to induce cytokine production by CD4 T cells of mice immunized with OVA–alum. CD4 T cells were cultured in the presence of OVA peptides as described in Experimental Procedures. Data represent mean cytokine concentration (pg/mL) and SE of triplicate cultures. ND, not detected.

microscope system, LSM410 (Carl Zeiss Co., Germany). Internalization of Alexa–OVA–red liposome conjugates in the macrophages was investigated in essentially the same manner as above.

Analysis of Three-Dimensional Structure of OVA. The three-dimensional structure of OVA reported by Stein et al. (*17*, *18*) was obtained from DBGET database links (http://www.genome.jp/dbget/), and the locations of the OVA peptides were displayed using ProteinAdviser (Fujitsu Kyusyu System Engineering Ltd., Fukuoka, Japan).

RESULTS

OVA Peptides Capable of Inducing Cytokine Production by OVA-Specific CD4$^+$ T Cells of BALB/c Mice. A series of sequentially synthesized OVA peptides shown in Table 1 were screened for the ability to induce cytokine production by CD4$^+$ T cells of BALB/c mice immunized with OVA–alum. Since, under the culture conditions described in Materials and Methods, no cytokine production was observed in the absence of OVA, nor by the use of CD4$^+$ T cells of naive BALB/c mice, the data shown in Table 2 were considered to represent antigen-specific cytokine production. In addition to well-known $OVA_{323-339}$, two OVA peptides, OVA_{20-43} and $OVA_{264-286}$, were found to induce significant production of all cytokines tested. The levels of cytokines induced by OVA_{20-43} and $OVA_{264-286}$ were even higher than those induced by $OVA_{323-339}$ in all cytokines tested. OVA_{20-43} involved the core motif of the I-A^d peptide-binding groove, OVA_{31-36}, but $OVA_{264-286}$ did not.

Cytokine Production by OVA-Specific CD4$^+$ T Cells Of Mice Immunized with OVA–Alum or OVA–Liposome, after Stimulation with OVA Peptides. The next attempt was performed using newly found OVA peptides, OVA_{20-43} and $OVA_{264-286}$, and a well-known OVA peptide, $OVA_{323-339}$. Splenic CD4$^+$ T cells were obtained from mice immunized either with OVA–liposome or OVA–alum and were cultured with OVA_{20-43}, $OVA_{264-286}$, or $OVA_{323-339}$ in the presence of APCs. As shown in Figure 1, the levels of cytokines produced by CD$^+$ T cells of mice immunized with OVA–liposome were significantly ($p < 0.01$) higher when the T cells were cultured either with OVA_{20-43} or $OVA_{323-339}$ than when they were cultured with $OVA_{264-286}$. On the other hand, in the culture of the CD4$^+$ T cells of mice immunized with OVA–alum, OVA_{20-43} and $OVA_{264-286}$ induced significantly higher levels of IL-5 and IFN-γ as compared to those induced by $OVA_{323-339}$, consistent with the results shown in Table 1. Similar results were obtained for the other cytokines, IL-2, IL-4, and IL-10 (data not shown).

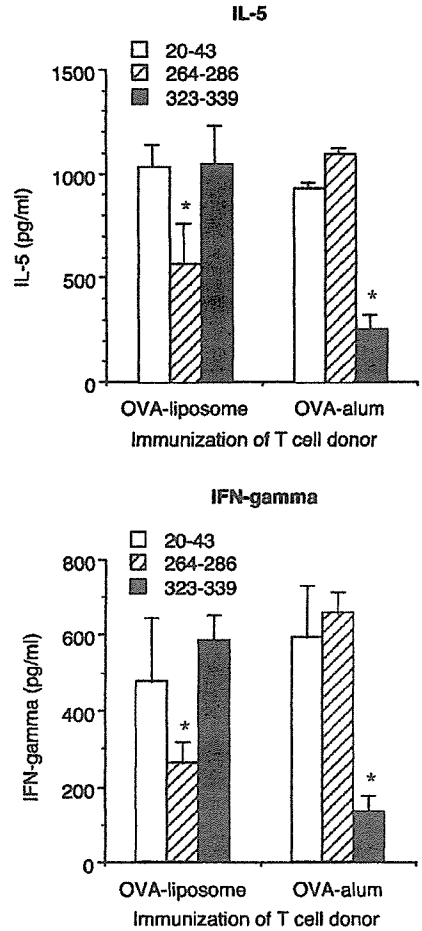

Figure 1. Cytokine production by CD4$^+$ T cells of mice immunized with OVA–liposome or OVA–alum, after in vitro stimulation with OVA peptides. CD4$^+$ T cells were taken from OVA-immune mice and cultured with OVA peptides as described in Materials and Methods. Data represent mean cytokine concentration (pg/mL) and SE of triplicate culture. Data are representative of three independent experiments.

Duration of Processing of Liposome-Coupled OVA in APCs. DQ–OVA coupled to liposome was cultured for 15 to 60 min with macrophage clone No. 39, and FACS analysis was performed. Figure 2a shows the fluorescence intensity of macrophages. A maximal processing of OVA was observed at 60 min. A consistent result was observed by confocal microscopic analysis (Figure 2b); the green fluorescence in the macrophages increased gradually within 60 min, suggesting that liposome-coupled OVA received processing significantly within 60 min after onset of the culture.

Internalization of Alexa–OVA–Red Liposome Conjugates in Macrophages. Alexa–OVA–red liposome conjugates, which appear yellow due to association with the green in Alexa–OVA and the red in the liposome, were cultured with macrophage clone No. 39 for 15 to 60 min, and confocal

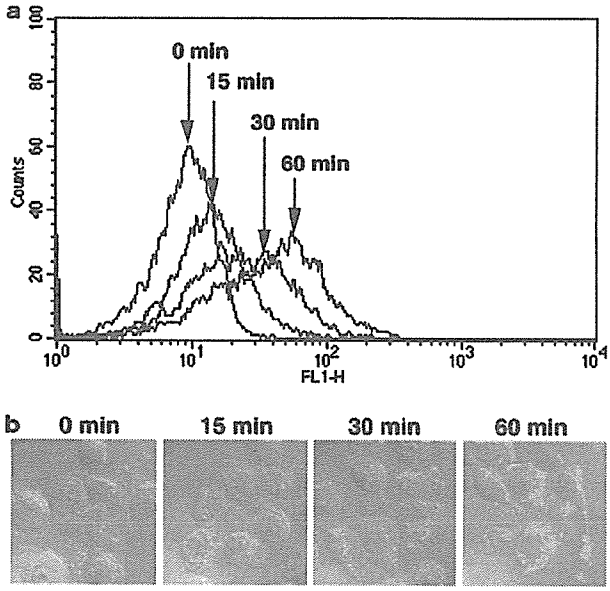

Figure 2. Digestion of liposome-coupled OVA by macrophages. DQ–OVA coupled to the surface of liposomes were added to the macrophage culture. Zero to 60 min after the onset of the culture, the macrophages were recovered and analyzed using flow cytometry (a) and confocal laser scanning microscopy (b).

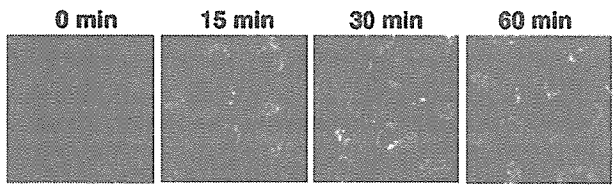

Figure 3. Association of OVA and liposomes in macrophages. Conjugates of Alexa488-labeled OVA and red-labeled liposomes were added to the macrophage culture. Zero to 60 min after the onset of the culture, the macrophages were recovered and analyzed using confocal laser scanning microscopy. The yellow spots observed in the macrophages are the result of the association with the Alexa488 (green) and red-labeled liposomes.

scanning microscopic analysis was performed. As shown in Figure 3, yellow spots were observed up to 60 min, suggesting that the OVA and liposomes were associated until liposome-coupled OVA received processing (Figure 2).

OVA Peptides in Three-Dimensional Structure of OVA. The locations of the three OVA peptides, OVA_{20-43}, $OVA_{264-286}$, and $OVA_{323-339}$, in the three-dimensional structure of OVA were analyzed. As shown in Figure 4, both $OVA_{264-286}$ and $OVA_{323-339}$ located on the surface of OVA in the three-dimensional structure, while OVA_{20-43} was situated inside the three-dimensional structure of OVA.

DISCUSSION

In the present study, OVA_{20-43} and $OVA_{264-286}$ were newly found among sequentially synthesized OVA peptides to stimulate $CD4^+$ T cells of OVA-immune BALB/c mice for cytokine production. A length of six residues has been proposed for core motifs of the I-A^d peptide-binding groove, with the first, third, and fourth residues being hydrophobic and the sixth generally being alanine or serine (*5*, *19*). OVA contains at least eight different epitopes with the I-A^d-binding motif, including $OVA_{327-332}$ which is involved in $OVA_{323-339}$. OVA_{20-43} involved core motifs of the I-A^d peptide binding groove, OVA_{31-36} and OVA_{32-37}, while $OVA_{264-286}$ did not. In addition, although OVA_{1-20}, OVA_{53-78}, $OVA_{220-245}$, and $OVA_{302-327}$

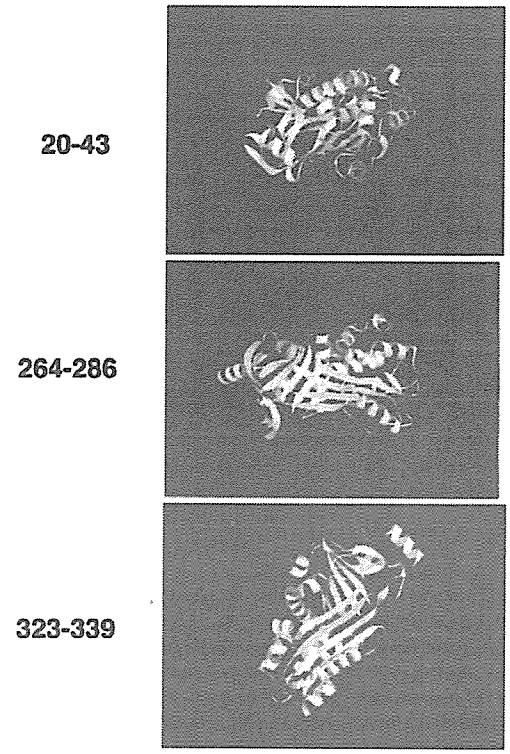

Figure 4. Location of OVA peptides in the three-dimensional structure of OVA. The OVA peptides in the three-dimensional structure of OVA are indicated as yellow strings.

involved the core motifs OVA_{1-6}, OVA_{63-68}, $OVA_{230-235}$, and $OVA_{312-317}$, respectively, none of them induced OVA-specific cytokine production by $CD4^+$ T cells of OVA-immune BALB/c mice (Table 2). These results suggest that the involvement of structural motifs of the MHC class II peptide binding groove in an antigenic peptide is not an essential condition for the activation of antigen-specific $CD4^+$ T cells. Also, regarding class I, although OVA contains six potential epitopes with the H-$2K^b$-binding motif (*20*), the CTL response is dominated by just one, $OVA_{257-264}$ (*21–23*). Thus, immunodominance would be directed by more than just the presence of an appropriate class I- or class II-binding motif.

The $\alpha\beta$ TCR comprises disulfide-linked α and β chains, each of which has a membrane-distal variable (Vα or Vβ) and membrane-proximal constant (Cα and Cβ) immunoglobulin superfamily (IgSF) domain, transmembrane regions, and short cytoplasmic segments (*24*). The peptide-MHC binding site is formed primarily from three complementary-determining regions (CDRs) or loops contributed by each Vα and Vβ domain. TCRs dock to the peptide-MHC in a topologically constrained manner, i.e., with the Vα domain of the TCR positioned over the N-terminal half of the peptide and the Vβ domain over the C-terminus (*25*, *26*). Thus, the shape of the TCR and/or peptide-MHC binding surfaces might limit the number of docking orientations (*24*). Therefore, the processing of both OVA_{20-43} and $OVA_{264-286}$ in APC to produce the "essential" length of the I-A^d-binding peptides sequence would be indispensable for the presentation of those peptides to $CD4^+$ T cells via the interaction between the peptide-MHC and TCRs.

Each Ia is considered to possess a single peptide binding site, based on the observation that unrelated peptides restricted by the same Ia molecule are capable of inhibiting the binding of one another to that particular Ia (*27*). This in turn supports the concept that a single site on Ia is capable of recognizing a structural motif common to many antigens (*5*). However, in the

present study, among two newly found I-A^d-binding OVA peptides, although each were found capable of stimulating antigen-specific $CD4^+$ T cells, one was demonstrated to involve a structural motif of the I-A^d peptide-binding groove but the other was not, suggesting the existence of another motif of the I-A^d peptide-binding groove.

$OVA_{323-339}$ induced a significantly higher level of cytokine production by $CD4^+$ T cells of mice immunized with OVA–liposome than that induced by $OVA_{264-286}$. However, in contrast, $OVA_{323-339}$ induced a significantly lower level of cytokine production by $CD4^+$ T cells of mice immunized with OVA–alum than that induced by $OVA_{264-286}$. These results suggest that the modification of OVA by the chemical coupling of OVA with liposomes may interrupt or alter antigen processing in APCs and result in the presentation of a differential set of peptides to T cells. In fact, the results of the present study demonstrated that the OVA and liposomes were associated until liposome-coupled OVA was processed (Figures 2 and 3). In the previous study (*13*), antigen–liposome conjugates were shown to be stable for at least 6 months if stored at 4 °C, and, if tetanus toxoid was coupled to liposomes and lyophilized, their efficacy was maintained for 6 months at 37 °C. The fact that both $OVA_{264-286}$ and $OVA_{323-339}$ were present on the surface of the three-dimensional structure of OVA made it reasonable to consider the effect of antigen-modification on the antigen processing in APCs. On the other hand, OVA_{20-43}, which induced a comparable level of cytokine production in both OVA–alum- and OVA–liposome-immune mice, was present inside the structure of OVA and likely not affected by the antigen-modification.

It is unlikely that the antigen-modification by the chemical coupling of antigen to liposomes detracts from the efficacy of vaccines when liposome-coupled antigen is applied to the vaccination protocol, since liposome-coupled toxins successfully induced protection against the tetanus toxin (*13*) or Shiga-like toxin (*14*, *28*, *29*) in mice (*13*, *14*) and also in monkeys (*28*). Nor it is unlikely that the difference between the two OVA peptides, $OVA_{264-286}$ and $OVA_{323-339}$, in the ability to induce cytokine production by $CD4^+$ T cells is reflected by the difference of immunodominance (i.e., affinity to bind I-A^d) in these two OVA peptides, since these peptides yielded opposite results in the stimulation of OVA-specific cytokine production by $CD4^+$ T cells of mice immunized by two different ways of immunization, i.e., OVA–alum and OVA–liposome. Thus, the results in the present study suggested that the modification of antigen affects antigen processing in APCs and results in the induction of differential T-cell epitopes as compared with those induced by plain antigen.

ACKNOWLEDGMENT

This work was supported in part by a grant from The Japan Health Sciences Foundation (Research on Health Sciences focusing on Drug Innovation).

LITERATURE CITED

(1) Chien, Y.-H., Jores, R., and Crowley, M. P. (1996) Recognition by γ/δ T cells. *Annu. Rev. Immunol. 14*, 511–532.

(2) Shimonkevitz, R., Colon, S., Kappler, J., Marrack, P. and Grey, H. M. (1984) Antigen recognition by H-2-restricted T cells. II. A tryptic ovalbumin peptide that substitutes for processed antigen. *J. Immunol.* 133, 2067–2074.

(3) Buus, S., Colon, S., Smith, C., Freed, J. H., Miles, C. and Grey, H. M. (1986) Interaction between a "processed" ovalbumin peptide and Ia molecules. *Proc. Natl. Acad. Sci. U.S.A. 83*, 3968–3971.

(4) Sette, A., Buus, S., Colon, S., Smith, J. A., Miles, C. and Grey, H. M. (1987) Structural characteristics of an antigen required for its interaction with Ia and recognition by T cells. *Nature 328*, 395–399.

(5) Sette, A., Buus, S., Colon, S., Miles, C. and Grey, H. M. (1988) I-A^d binding peptides derived from unrelated protein antigens share a common structural motif. *J. Immunol. 141*, 45–48.

(6) Sette, A., Buus, S., Appella, E., Smith, J. A., Chesnut, R., Miles, C., Colon, S. M., and Grey, H. M. (1989) Prediction of major histocompatibility complex binding regions of protein antigens by sequence pattern analysis. *Proc. Natl. Acad. Sci. U.S.A. 86*, 3296–3300.

(7) Sette, A., Buus, S., Colon, S., Miles, C. and Grey, H. M. (1989) Structural analysis of peptides capable of binding to more than one Ia antigen. *J. Immunol. 142*, 35–40.

(8) Sette, A., Lamont, A., Buus, S., Colon, S. M., Miles, C. and Grey, H. M. (1989) Effect of conformational propensity of peptide antigens in their interaction with MHC class II molecules: failure to document the importance of regular secondary structures. *J. Immunol. 143*, 1268–1273.

(9) Sette, A., Sidney, J., Albertson, M., Miles, C., Colon, S. M., Pedrazzini, T., Lamont, A. G. and Grey, H. M. (1990) A novel approach to the generation of high affinity class II-binding peptides. *J. Immunol. 145*, 1809–1813.

(10) Naito, S., Horino, A., Nakayama, M., Nakano, Y., Nagai, T., Mizuguchi, J., Komuro, K., and Uchida, T. (1996) Ovalbumin-liposome conjugate induces IgG but not IgE antibody production. *Int. Arch. Allergy Immunol. 109*, 223–228.

(11) Nakano, Y., Mori, M., Nishinohara, S., Takita, Y., Naito, S., Horino, A., Kato, H., Taneichi, M., Komuro, K., and Uchida, T. (1999) Antigen-specific, IgE-selective unresponsiveness induced by antigen-liposome conjugates: Comparison of four different conjugation methods. *Int. Arch. Allergy Immunol. 120*, 199–208.

(12) Nakano, Y., Mori, M., Nishinohara, S., Takita, Y., Naito, S., Kato, H., Taneichi, M., Komuro, K., and Uchida, T. (2001) Surface-linked liposomal antigen induces IgE-selective unresponsiveness regardless of the lipid components of liposomes. *Bioconjugate Chem. 12*, 391–395.

(13) Naito, S., Horino, A., Komiya, T., Fukuda, T., Takahashi, M., Ami, Y., Suzaki, Y., Oka, T., Okuma, K., Morokuma, M., Nakano, Y., Mori, M., Nishinohara, S., Komuro, K., and Uchida, T. (1998) Induction of protection against tetanus toxin in mice by tetanus toxoid-liposome conjugate. *Int. Arch. Allergy Immunol. 116*, 215–219.

(14) Fukuda, T., Komiya, T., Takahashi, M., Arakawa, Y., Ami, Y., Suzaki, Y., Naito, S., Horino, A., Nagata, N., Satoh, S., Gondaira, F., Sugiyama, J., Nakano, Y., Mori, M., Nishinohara, S., Komuro, K., and Uchida, T. (1998) Induction of protection against oral infection with cytotoxin-producing Escherichia coli O157: H7 in mice by Shiga-like toxin-liposome conjugate. *Int. Arch. Allergy Immunol. 116*, 313–317.

(15) Tanaka, Y., Kasai, M., Taneichi, M., Naito, S., Kato. H., Mori, M., Nishida, M., Maekawa, N., Yamamura, H., Komuro, K., and Uchida, T. (2004) Liposomes with differential lipid components exert differential adjuvanticity in antigen-liposome conjugates via differential recognition by macrophages. *Bioconjugate Chem. 15*, 35–40.

(16) Uchida, T., Ju, S. T., Fay, A., Liu, Y. N. and Dorf, M. E. (1985) Functional analysis of macrophage hybridomas. I. Production and initial characterization. *J. Immunol. 134*, 772–778.

(17) Stein, P. E., Leslie, A. G. W., Finch, J. T., Turnell, W. G., Mclaughlin, P. J., and Carrell, R. W. (1990) Crystal structure of ovalbumin as a model for the reactive centre of serpins. *Nature 347*, 99–102.

(18) Stein P. E., Leslie, A. G., Finch, J. T., and Carrel, R. W. (1991) Crystal structure of uncleaved ovalbumin at 1.95A resolution. *J. Mol. Biol. 221*, 941–959.

(19) Scott, C. A., Peterson, P. A., Teyton, L. and Wilson, I. A. (1998) Crystal structures of two I-A^d-peptide complexes reveal that high affinity can be achieved without large anchor residues. *Immunity 8*, 319–329.

(20) Jameson, S. C., and Bevan, M. J. (1988) Dissection of major histocompatibility complex (MHC) and T cell receptor contact residues in a K^b-restricted ovalbumin peptide and an assessment of the predictive power of MHC-binding motifs. *Eur. J. Immunol. 22*, 2663–2667.

(21) Moor, M. W., Carbone, F. R., and Bevan, M. J. (1988) Introduction of soluble protein into the class I pathway of antigen processing and presentation. *Cell 54*, 777–785.

(22) Rotzschke, O., Falk, K., Stevanovic, G., Walden, P., and Ramensee, H. G. (1991) Exact prediction of a natural T cell epitope. *Eur. J. Immunol, 21*, 2891−2894.
(23) Kim, D. T., Mitchell, D. J., Brockstedt, D. G., Fong, L., Nolan, G. P., Fathman, C. G., Engleman, E. G., and Rothbard, J. B. (1997) Introduction of soluble proteins into the MHC class I pathway by conjugation to an HIV *tat* peptide. *J. Immunol. 159*, 1666−1668.
(24) Anton van der Merwe, P., and Davis, S. J. (2003) Molecular interactions mediating T cell antigen recognition. *Annu. Rev. Immunol. 21*, 659−684.
(25) Hennecke, J., and Wiley, D. C. (2001) T cell receptor-MHC interactions up close. *Cell 104*, 1−4.
(26) Rudolph, M. G., and Wilson, I. A. (2002) The specificity of TCR/pMHC interaction. *Curr. Opin. Immunol. 14*, 52−65.
(27) Buus, S., Sette, A., Colon, S., Miles, C., and Grey, H. M. (1987) The relation between MHC restriction and the capacity of Ia to bind immunogenic peptides. *Science 235*, 1353−1357.
(28) Suzaki, Y., Ami, Y., Nagata, N., Naito, S., Kato, H., Taneichi, M., Takahashi, M., Komiya, T., Satoh, S., Gondaira, F., Sugiyama, J., Nakano, Y., Mori, M., Komuro, K., and Uchida, T. (2002) Protection of monkeys against Shiga toxin induced by Shiga toxin-liposome conjugates. *Int. Arch. Allergy Immunol. 127*, 294−298.
(29) Uchida, T. (2003) Stx-liposome conjugates as candidate vaccines. *Drugs Today 39*, 673−693.

BC060024G

Antigen Chemically Coupled to the Surface of Liposomes Are Cross-Presented to CD8$^+$ T Cells and Induce Potent Antitumor Immunity[1]

Maiko Taneichi,* Hideaki Ishida,† Kiichi Kajino,† Kazumasa Ogasawara,† Yuriko Tanaka,* Michiyuki Kasai,* Masahito Mori,‡ Mitsuhiro Nishida,‡ Hiroyuki Yamamura,‡ Junichiro Mizuguchi,§ and Tetsuya Uchida[2]*

We have previously demonstrated that liposomes with differential lipid components display differential adjuvant effects when Ags are chemically coupled to their surfaces. In the present study, Ag presentation of liposome-coupled OVA was investigated in vitro, and it was found that OVA coupled to liposomes made using unsaturated fatty acid was presented to both CD4$^+$ and CD8$^+$ T cells, whereas OVA coupled to liposomes made using saturated fatty acid was presented only to CD4$^+$ T cells. Confocal laser scanning microscopic analysis demonstrated that a portion of the OVA coupled to liposomes made using unsaturated, but not saturated fatty acid, received processing beyond the MHC class II compartment, suggesting that the degradation of OVA might occur in the cytosol, and that the peptides generated in this manner would be presented to CD8$^+$ T cells via MHC class I. The ability to induce cross-presentation of an Ag coupled to liposomes consisting of unsaturated fatty acid was further confirmed by in vivo induction of CTL and by the induction of tumor eradication in mice; E.G7 tumors in mice that received combined inoculation with $OVA_{257-264}$-liposome conjugates, CpG, and anti-IL-10 mAbs were completely eradicated. In those mice, the frequency of CD8$^+$ T cells reactive with $OVA_{257-264}$ peptides in the context of H-2K^b was significantly increased. These results suggested that, by choosing lipid components for liposomes, surface-coupled liposomal Ags might be applicable for the development of tumor vaccines to present tumor Ags to APCs and induce antitumor responses. *The Journal of Immunology,* **2006, 177: 2324–2330.**

Although it has long been a matter of debate whether the human immune system is capable of recognizing and managing spontaneously arising tumors, a number of compelling findings (1–4) have recently indicated that the immune system is clearly capable of recognizing and eliminating tumor cells. Therefore, adoptive immunotherapy could potentially provide a controlled and highly specific stratagem for the treatment of cancer. However, at present, there are some problems to overcome before immunotherapy can be applied to cancer therapies. Successful elimination of experimental tumors in animal models by use of adoptive immunotherapy requires repeated administration of IL-2 to maintain cell survival because, for solid cancers, the capacity of tumor rejection may soon be exhausted unless CTL are rapidly and efficiently recruited to the tumor bed. Also, in humans, adoptive immunotherapy has been (5) plagued by extreme toxicities associated with the simultaneous administration of high doses of IL-2. Second, most of the characterized human tumor Ags have been classified as tumor-associated, because of their demonstrable expression at low levels in some normal cells (6). Thus, the challenge for immunotherapy is to develop strategies that effectively and safely augment antitumor responses (7).

Immunotherapy for the treatment of cancer involves adoptive T cell transfer, tumor-associated-Ag-pulsed dendritic cells (DC[3]; DC-based vaccines), and peptide-based vaccines. In the case of the peptide-based cancer vaccines, the vaccine Ag (e.g., tumor Ag) should be presented via the MHC class I pathway for the induction of Ag-specific CTL. In general, extracellular Ags are presented via MHC class II molecules to CD4$^+$ T cells, whereas intracellular Ags are presented via MHC class I molecules to CD8$^+$ T cells. To induce Ag-specific CTL, the tumor Ag must be loaded onto the class I MHC processing pathway in the APCs via so-called cross-presentation (8). In cross-presentation, exogenous proteins cross over to the endogenous pathway to gain access to MHC class I. Using this phenomenon, a generation of Ag-specific, primary CD8$^+$ CTL responses might be applicable for the development of vaccines for prevention of viral diseases and for the induction of potent protective antitumor immunity.

As for the vaccine adjuvant, the currently approved alum adjuvants are known to be effective only for the induction of humoral immunity, not for the induction of cell-mediated immunity (9–11). Consequently, the development of a novel vaccine adjuvant is essential for the induction of cell-mediated immunity. Among the candidates for adjuvants, liposomes have garnered recent attention (12–18) for their capacity as carriers of vaccines. We previously (19–22) reported that Ags chemically coupled to the surface of liposomes induced Ag-specific IgG but not IgE Ab production.

*Department of Safety Research on Blood and Biological Products, National Institute of Infectious Diseases, Tokyo, Japan; †Department of Pathology, Shiga University of Medical Science, Shiga, Japan; ‡Drug Delivery System Development Division, Nippon Oil and Fat Corporation, Tokyo, Japan; and §Department of Immunology, Tokyo Medical University, Tokyo, Japan

Received for publication December 29, 2005. Accepted for publication May 24, 2006.

The costs of publication of this article were defrayed in part by the payment of page charges. This article must therefore be hereby marked *advertisement* in accordance with 18 U.S.C. Section 1734 solely to indicate this fact.

[1] This work was supported in part by a grant from the Japan Health Sciences Foundation (Research on Health Sciences focusing on Drug Innovation).

[2] Address correspondence and reprint requests to Dr. Tetsuya Uchida, Department of Safety Research on Blood and Biological Products, National Institute of Infectious Diseases, 4-7-1 Gakuen, Musashimurayama-city, Tokyo, Japan. E-mail address: tuchida@nih.go.jp

[3] Abbreviations used in this paper: DC, dendritic cell; DPPE, dipalmitoyl phosphatidyl ethanolamine; DOPE, dioleoyl phosphatidyl ethanolamine; DSS, disuccinimidyl suberate; SAC, splenic adherent cells; TAA, antitumor-associated Ag.

0022-1767/06/$02.00

The inducibility of Ag-specific IgG Ab production by Ag-liposome conjugates varied among the liposome preparations used for the production of Ag-liposome conjugates; the greater the membrane mobility in liposomes, the more Ab production induced by Ag-liposome conjugates (23). In fact, alteration of lipid composition has been reported to modulate immune responses (24–27).

In the present study, OVA was coupled to liposomes consisting either of saturated or unsaturated fatty acid, and the inducibility of cross-presentation by these OVA-liposome conjugates was investigated by monitoring in vitro cytokine production by OVA-specific $CD4^+$ or $CD8^+$ T cells cocultured with Ag-liposome conjugates in the presence of APCs. OVA coupled to liposomes consisting of unsaturated fatty acid was presented to both $CD4^+$ and $CD8^+$ T cells. We then made conjugates of $OVA_{257-264}$ with liposomes consisting of unsaturated fatty acid, and investigated in vivo CTL induction and the effect of administrating these conjugates to E.G7-bearing mice.

Materials and Methods

Mice

BALB/c mice (8 wk of age, female) were purchased from Charles River Laboratories. C57BL/6 mice (6–8 wk of age, female) were purchased from SLC (Shizuoka, Japan). All mice were maintained under specific pathogen-free conditions.

Chemicals

All phospholipids were obtained from Nippon Oil and Fat. Reagent grades of cholesterol were purchased from Wako Pure Chemical.

Reagents

Synthetic CpG ODN (5002: TCCATGACGTTCTTGATGTT) was purchased from Hokkaido System Science and was phoshorothioate protected to avoid nuclease-dependent degradation. Mouse MHC class-I (K^b)-binding peptide $OVA_{257-264}$ (SIINFEKL) was also obtained from Hokkaido System Science. FITC-conjugated anti-mouse CD8 mAb or PE-conjugated $H\text{-}2K^b/OVA_{257-264}$ tetramer was purchased from BD Biosciences or MBL, respectively.

Antigens

OVA (grade VII) was purchased from Sigma-Aldrich. For the analysis of the processing of liposome-coupled OVA by macrophages, DQ-OVA, which exhibits green fluorescence upon proteolytic degradation, was purchased from Molecular Probes.

Fluorescence labeling of OVA

OVA was labeled with fluorescence using an AlexaFluor 488 protein labeling kit (Molecular Probes) according to the manufacturer's protocol.

Liposomes

Liposomes with two different lipid components were used in the present study. Saturated liposomes consisted of dipalmitoyl phosphatidylcholine, dipalmitoyl phosphatidyl ethanolamine (DPPE), dimyristoyl phosphatidyl glycerol, and cholesterol in a 4:3:2:7 molar ratio, and unsaturated liposomes consisted of dioleoyl phosphatidylcholine, dioleoyl phosphatidyl ethanolamine (DOPE), dioleoyl phosphatidyl glycerol, and cholesterol in a 4:3:2:7 molar ratio. The crude liposome solution was passed through a membrane filter (Nucleopore polycarbonate filter; Costar) with a pore size of 0.2 μm.

Coupling of OVA to liposomes

Liposomal conjugates with plain OVA, Alexa-labeled OVA, or DQ-OVA were prepared essentially in the same way, as described previously (19), via glutaraldehyde. Briefly, 6 mg of OVA in 2.5 ml of phosphate buffer (pH 7.2) was added to a mixture of 90 mg of liposomes, in a dropwise fashion, and 0.5 ml of 2.5% glutaraldehyde solution. The mixture was stirred gently for 1 h at 37°C and then 0.5 ml of 3 M glycine-NaOH (pH 7.2) was added to block excess aldehyde groups. This was followed by incubation overnight at 4°C. The liposome-coupled OVA and uncoupled OVA in the resulting solution were separated using CL-4B column chromatography (Pharmacia). The amount of lipid in the liposomal fraction was measured using a Phospholipid-Test-Wako phospholipid content assay kit (Wako Pure Chemical). The OVA-liposome solution was adjusted to 10 mg lipid/ml in RPMI 1640, sterile-filtered using a Millex-HA syringe filter unit (0.45 μm; Millipore), and kept at 4°C until use.

Coupling of $OVA_{257-264}$ to liposomes

Liposomal conjugates with $OVA_{257-264}$ were prepared essentially in the same way as described previously (20) via disuccinimidyl suberate (DSS). Briefly, a mixture of 10 ml of anhydrous chloroform solution containing 0.136 mM DPPE (saturated liposomes) or DOPE (unsaturated liposomes) and 24 μl of triethylamine was added in drops to 26.6 ml of anhydrous chloroform solution containing 0.681 mM DSS and stirred for 5 h at 40°C. The solvent was evaporated under reduced pressure, and 18 ml of a 2:1 mixture of ethyl acetate and tetrahydrofuran was added to dissolve the residue. Thirty six milliliters of 100 mM sodium phosphate (pH 5.5) and 90 ml of saturated NaCl aqueous solution were added to the solution, shaken for 1 min, and allowed to separate. To remove undesirable materials, the upper layer was washed with the same buffer and, after evaporation of the solvent, 3 ml of acetone was added to dissolve the residue. Ice-cold acetone (100 ml) was added in drops and kept on ice for 30 min to precipitate. Crystals were collected and dissolved in 5 ml of chloroform. After evaporation, 34.4 mg of DPPE-DSS was obtained. 0.18 mM dipalmitoyl phosphatidylcholine, 0.03 mM DPPE-DSS, 0.21 mM cholesterol, and 0.06 mM dimyristoyl phosphatidyl glycerol were dissolved in 10 ml of chloroform/methanol (saturated liposomes). For unsaturated liposomes, DOPE-DSS, dioleoyl phosphatidylcholine, dioleoyl phosphatidyl glycerol, and cholesterol were used and the preparation was done in the same manner as above. The solvent was then removed under reduced pressure and 5.8 ml of phosphate buffer (pH 7.2) was added to make a 4.8% lipid suspension. The vesicle dispersion was extruded through a 0.2-μm polycarbonate filter to adjust the liposome size. A 2-ml suspension of DSS-introduced liposome and 0.5 ml of 5 mg/ml $OVA_{257-264}$ solution were mixed and stirred for 3 days at 4°C. The liposome-coupled and -uncoupled peptides were separated as described above using CL-4B column chromatography.

Quantification of OVA coupled to liposome

For the measurement of OVA coupled to liposome, radiolabeled OVA (*methyl*-^{14}C; purchased from New England Nuclear) was mixed with cold OVA and used for coupling with liposome and for determining the calibration curve. The radioactivity of the resulting OVA-liposome solution was counted using a calibration curve. The amounts of OVA coupled to saturated and unsaturated liposomes were 48.1 and 47.8 μg/mg lipid, respectively.

Cell culture

All incubations were performed in RPMI 1640 (Invitrogen Life Technologies) supplemented with 10% heat-inactivated FCS (HyClone), 100 U/ml penicillin, and 100 μg/ml streptomycin (Invitrogen Life Technologies).

Preparation of splenic adherent cells (SAC) and $CD4^+$ and $CD8^+$ T cells

Spleen cell suspensions were prepared in RPMI 1640 containing 10% FCS. Cells (5×10^7) in 5 ml of medium containing 10% FCS were plated into 50-mm plastic tissue culture dishes (no. 3002; BD Biosciences) and were incubated at 37°C in a humidified 5% CO_2 atmosphere for 2 h. After culture, nonadherent cells were removed by vigorous washing in warm medium, and adherent cells were then harvested with a cell scraper. $CD4^+$ and $CD8^+$ T cell purification from spleen cells of mice immunized with OVA-alum was performed with the magnetic cell sorter system MACS according to the manufacturer's protocol using anti-CD4 and anti-CD8 Ab-coated microbeads (Miltenyi Biotec). T cells were suspended in RPMI 1640 containing 10% FCS at a cell density of 2×10^6/ml.

Culture of $CD4^+$ and $CD8^+$ T cells with SAC pulsed with OVA

OVA-liposome conjugates made using saturated or unsaturated liposomes were added to the culture of SAC and incubated for 2 h. The final concentration of OVA-liposome added to the macrophage culture was 500 μg of lipid/ml, which included 24 μg of OVA/ml. For controls, OVA was added to the culture at final concentrations of 24 μg/ml. SAC were then washed three times in ice-cold medium and 2×10^5 cells were cocultured with 5×10^5 $CD4^+$ or $CD8^+$ T cells in a 48-well plate (no. 3047; BD Biosciences). A preliminary experiment showed that the optimal culture period in the above culture condition was 2 days for IFN-γ production by $CD4^+$ T cells and 5 days for IL-5 production by $CD4^+$ and $CD8^+$ T cells

and IFN-γ production by $CD8^+$ T cells. After incubation in a CO_2 incubator for 2 or 5 days, the culture supernatants were collected and assayed for cytokines.

Cytokine assays

IL-5 and IFN-γ in the culture supernatant were measured using the Biotrak mouse ELISA system (Amersham International). All test samples were assayed in duplicate, and the SE in each test was always <5% of the mean value.

Cloned macrophage hybridoma

Macrophage hybridoma clone 39, obtained from the fusion of SAC from CKB mice and P388D1 (28), was maintained in RPMI 1640 supplemented with 10% heat-inactivated FCS, 100 U/ml penicillin, and 100 μg/ml streptomycin in a 75-cm^2 flask (no. 3111; BD Biosciences).

Construction and expression of a fusion protein, DM-DsRed, in macrophage clone 39

The DNA fragment coding the full-length H2-DMβ2 (29) was amplified by PCR with two primers (5′-ATGGCTGCACTCTGGCTGCTGCTGCT GGT-3′ and 5′-GATGCCGTCCTTCTGGGTAGGTGGATCC-3′). The PCR product was cloned into the CMV promoter-driven expression plasmid pDsRedN1 (BD Clontech). This construct omitted the stop codon of H2-DMβ2 and encoded the H2-DMβ2 fused with DsRed. The cloned plasmid DNA was transfected to macrophage hybridoma clone 39 with Effectene transfection reagent (Qiagen) according to the manufacturer's protocol. During the transfection to clone 39, the medium containing cDNA and the transfection reagent was replaced with fresh medium after an 8-h transfection, and then clone 39 was cultured for 40 h. To obtain stable cell lines, clone 39 was passaged at 1:5 into RPMI 1640 containing 10% FCS with 50 μg/ml geneticin (G-418; Sigma-Aldrich). Cells showing the best fluorescence were selected by using a FACSVantage cell sorter. After cell sorting, clone 39 that expressed DM-DsRed was cultured in RPMI 1640 containing 10% FCS with 200 μg/ml geneticin.

Confocal laser scanning microscopy

To investigate the internalization of OVA-liposome conjugates by macrophages, the DM-DsRed-expressing cloned macrophages 39 were cultured for 18 h at 37°C on 8-hole heavy Teflon-coated slides (Bokusui Brown) and was then incubated with Alexa-OVA-liposome conjugates or with DQ-OVA-liposome conjugates, prepared using saturated or unsaturated liposomes, for 2 h at 37°C. The slides were then washed with MEM and fixed with 4% paraformaldehyde in PBS for 10 min at room temperature. After fixation, they were incubated for 10 min in 0.1 M glycine-HCl (pH 7.0) to block the remaining aldehyde residue. They were then washed two times in PBS. After washing, the slides were sealed with PBS:glycerin (1:9) and analyzed under an LSM410 confocal laser scanning microscope system (Zeiss).

In vivo cytotoxicity assay

Splenocytes of C57BL/6 mice were labeled with either 0.5 or 5 μM carboxylfluorescein diacetate succinimidyl ester (Sigma-Aldrich) for 15 min at room temperature and washed twice. $CFSE^{bright}$ cells (M2) were subsequently pulsed with 0.5 μg/ml $OVA_{257-264}$ for 90 min at 37°C. $CFSE^{dull}$ cells (M1) were pulsed with irrelevant $NP_{366-374}$ (ASNENMDAM) peptide for 90 min at 37°C as a control. Cells were mixed at a 1:1 ratio, and then a total of 5×10^6 cells was injected i.v. into mice that had been injected 1 wk earlier with 100 μg of the anti-IL-10 mAb 2A5 (30), 5 μg of CpG, and the indicated liposomal Ags. Eight hours later, splenocytes from each mouse were analyzed by flow cytometry.

Tumor cells

E.G7 cells, generated by transducing the chicken OVA gene into the murine lymphoma cell line EL4, were purchased from American Type Culture Collection.

Tumor challenge experiment

Female C57BL/6 mice were inoculated s.c. in the right flank with 1×10^6 E.G7 cells. When the tumor mass had grown to 5 mm in diameter, the mice were injected with 100 μg of anti-IL-10 mAbs and 5 μg of CpG with or without 200 μl of liposome-coupled $OVA_{257-264}$. The same treatment was repeated 2 days later. The size of the tumor mass was measured every day, and the average diameter of the tumor mass in each group was calculated. Inoculation of anti-IL-10 mAbs and CpG without $OVA_{257-264}$ in the condition used in the present study did not affect growth of E.G7 in mice.

Cellular staining with MHC tetramer

Spleen cells from tumor-bearing mice with or without the treatment were treated with anti-FcγRII/III mAb (2.4G2) and then stained with FITC-conjugated anti-CD8 mAb and PE-conjugated $H\text{-}2K^b/OVA_{257-264}$ tetramer at room temperature for 30 min. After two washes in PBS, cells were examined to quantify OVA-specific CTL by flow cytometry. Flow cytometric analyses were performed using a FACScan flow cytometer (BD Biosciences). Data were presented as dot plots using CellQuest software (BD Biosciences).

Statistical analysis

The Student's *t* test was used for the statistical analysis.

Results

Cytokine production by splenic $CD4^+$ and $CD8^+$ T cells of mice immunized with OVA after coculture with OVA-pulsed SAC

Splenic adherent cells of BALB/c mice were cocultured with OVA-liposome conjugates made using liposomes with two different lipid components for 2 h. The donor mice used as a source of $CD4^+$ and $CD8^+$ T cells in this experiment were immunized with OVA-alum, since in the preliminary experiment, $CD8^+$ T cells of C57BL/6 mice immunized with OVA-alum responded significantly to in vitro stimulation with $OVA_{257-264}$, a mouse MHC class I (K^b)-binding peptide, and produced cytokines such as IL-5 and IFN-γ in an Ag-specific manner. As shown in Table I, OVA-liposome conjugates made using liposomes with two different lipid components induced production of comparable levels of IL-5 and IFN-γ by $CD4^+$ T cells, whereas OVA solution with the same Ag concentration as OVA-liposome induced a much lower level of IL-5 production and no IFN-γ. In contrast, OVA-liposomes made using saturated liposomes did not induce either IL-5 or IFN-γ production by $CD8^+$ T cells, whereas OVA-liposomes made using unsaturated liposomes induced a significant production of both IL-5 and IFN-γ.

Confocal laser scanning microscopic analysis of macrophages cocultured with Alexa-OVA-liposome or with DQ-OVA-liposome conjugates

Alexa-labeled OVA was coupled with liposomes of two different lipid components and added to the culture of cloned macrophages

Table I. *Cytokine production by splenic CD4/CD8 T cells of mice immunized with OVA after coculture with OVA-pulsed SAC*[a]

In Vitro Ag	Liposomes	CD4		CD8	
		IL-5	IFN-γ	IL-5	IFN-γ
None		ND	ND	ND	ND
OVA solution		96.2 ± 12.5	ND	ND	ND
OVA-liposome	Saturated	910.2 ± 23.0	88.7 ± 45.0	ND	ND
OVA-liposome	Unsaturated	1065.5 ± 31.9	115.1 ± 28.6	163.3 ± 99.1	149.9 ± 83.8

[a] Splenic CD4/CD8 T cells were taken from mice immunized with OVA and were cultured with OVA-pulsed SAC as described in *Materials and Methods*. Data represent the mean cytokine concentration (picograms per milliliter) in the culture supernatants and SE of triplicate culture. ND, Not detected.

that expressed DM-DsRed. After incubation for 2 h, the recovered macrophages were analyzed using confocal laser scanning microscopy. Macrophages expressed DM-DsRed (Mϕ alone in Figs. 1 and 2). The yellow spots in the panel labeled saturated in Fig. 1 illustrate that Alexa-OVA coupled to liposomes were colocalized with DM. In contrast, in the panel labeled unsaturated in Fig. 1, both green and yellow spots were observed, suggesting that a portion of the Alexa-OVA coupled to unsaturated liposomes was not colocalized with DM. In the next experiment, DQ-OVA, which exhibits green fluorescein upon proteolytic degradation, was coupled to liposomes instead of Alexa-OVA, and similar investigations were performed. Interestingly, the results shown in Fig. 2 demonstrate that a portion of the DQ-OVA coupled to unsaturated liposome received processing beyond the class II compartment.

In vivo CTL induction by OVA-liposome conjugates

Cross-presentation of OVA coupled to unsaturated liposomes was further confirmed using experiments of in vivo CTL induction. As shown in Fig. 3, both $OVA_{257-264}$ (*D*) and whole OVA (*E*) coupled to unsaturated liposomes successfully induced CTL against target cells pulsed with $OVA_{257-264}$ but not with control $NP_{366-374}$. In contrast, a mixture of $OVA_{257-264}$ and unsaturated liposomes (Fig. 3*B*), and $OVA_{257-264}$ coupled to saturated liposome (Fig. 3*C*) failed to induce CTL against target cells pulsed with $OVA_{257-264}$.

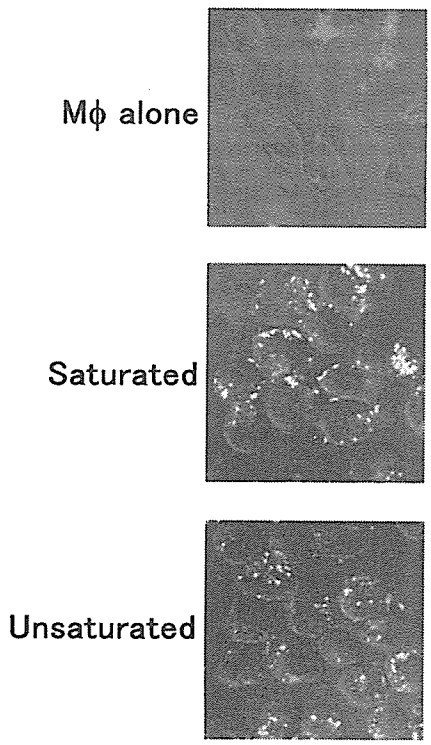

FIGURE 1. Confocal laser scanning microscopic analysis of macrophages cocultured with Alexa-OVA-liposome conjugates. DM-DsRed-expressing macrophages were cocultured with Alexa-OVA-liposome made using saturated or unsaturated liposomes, as described in *Materials and Methods*. Two hours after the onset of the culture, macrophages were recovered and analyzed using confocal laser scanning microscopy. These optically merged images are representative of most cells examined by confocal microscopy. Yellow, colocalization of green (Alexa-OVA) and red (macrophage DM); Mϕ alone, macrophages without coculture with Alexa-OVA-liposome.

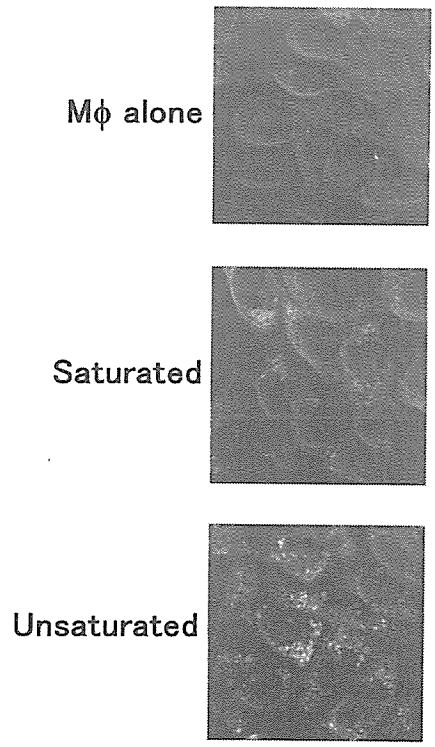

FIGURE 2. Confocal laser scanning microscopic analysis of macrophages cocultured with DQ-OVA-liposome conjugates. DM-DsRed-expressing macrophages were cocultured with DQ-OVA-liposome made using saturated or unsaturated liposomes, as described in *Materials and Methods*. Two hours after the onset of the culture, macrophages were recovered and analyzed using confocal laser scanning microscopy. These optically merged images are representative of most cells examined by confocal microscopy. Yellow, colocalization of green (DQ-OVA received processing) and red (macrophage DM); Mϕ alone, macrophages without coculture with DQ-OVA-liposome.

Tumor-specific, liposome-coupled Ag peptides induce eradication of tumors in C57BL/6 mice

To examine the effectiveness of liposome-coupled peptides in vivo, we performed tumor-rejecting experiments. B6 mice were injected s.c. with E.G7 cells transfected with OVA DNA, and solid tumors with a diameter of >5 mm were established ~7–10 days after the injection. Liposome-coupled peptides, $OVA_{257-264}$ with CpG and anti-IL-10 Ab, were injected twice around the tumor mass as described in *Materials and Methods*. As shown in Fig. 4, a significant ($p < 0.001$) decrease of mean tumor diameter was observed as early as 7 days after inoculation of liposome-coupled $OVA_{257-264}$ with CpG and anti-IL-10 Ab, and the tumors were completely eradicated in 12 days. In contrast, injection of CpG and anti-IL-10 Ab with peptide solution containing the same amount of $OVA_{257-264}$ as liposome-coupled $OVA_{257-264}$ did not eradicate the established tumors. These results suggested that the liposome-coupled $OVA_{257-264}$ might effectively present $OVA_{257-264}$ to CTL, resulting in tumor rejection.

To determine whether liposome-coupled $OVA_{257-264}$ contributes to CTL activation, we analyzed splenic T cells in tumor-bearing mice with or without the treatment. CD8-gated cells were analyzed with a tetramer-detecting $OVA_{257-264}$ plus H-$2K^b$-specific T cells. As shown in Fig. 5, spleen cells in normal mice were slightly stained with the tetramer at a background level. The tetramer-positive cells accounted for 5.2% of the total $CD8^+$ cells of tumor-eradicated mice, whereas they made up 1.8 and 2.3% in normal mice and nontreated, tumor-bearing mice, respectively.

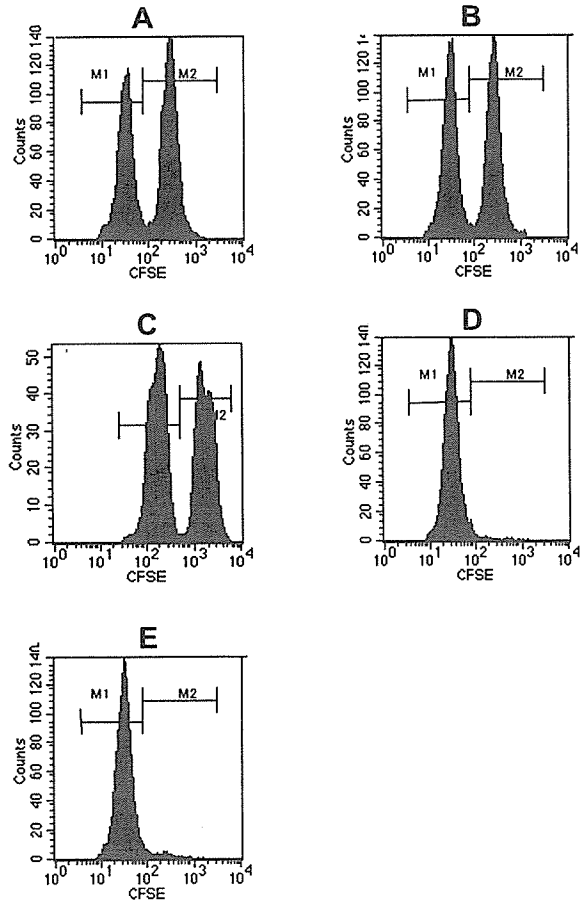

FIGURE 3. In vivo CTL induction in mice immunized with OVA-liposome conjugates. Mice were injected with 100 μg of anti-IL-10 mAbs and 5 μg of CpG with PBS (*A*), a mixture of $OVA_{257-264}$ and unsaturated liposomes (*B*), $OVA_{257-264}$-saturated liposome conjugates (*C*), $OVA_{257-264}$-unsaturated liposome conjugates (*D*), and OVA-unsaturated liposome conjugates (*E*). Target cells were prepared as described in *Materials and Methods*. $CFSE^{bright}$ cells (M2) were pulsed with $OVA_{257-264}$, and $CFSE^{dull}$ cells (M1) were pulsed with $NP_{366-374}$ peptide as a control. Data represent the results of flow cytometric analysis for splenocytes from each mouse.

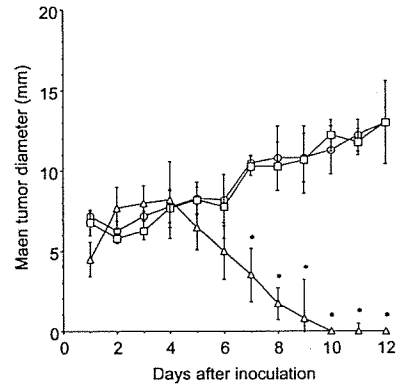

FIGURE 4. The effect of peptide-liposome conjugates on the growth of E.G7 tumor in mice. The tumor was established as explained in *Materials and Methods*, and a mixture of CpG and anti-IL-10 were inoculated around the tumor mass with liposome-coupled peptide (△), peptide solution containing the same amount of peptide as liposome-coupled peptide (□), or with nothing (○). *, $p < 0.001$ as compared with the mean diameter of mice without inoculation of liposome-coupled peptides. Data represent the mean and SE of four mice per group.

Discussion

In most APCs, exogenous Ags cannot be presented by the MHC class I because the exogenous Ags are unable to gain access to the cytosolic compartment. This segregation of exogenous Ags from the class I pathway is important to prevent CTL from killing health cells that have been exposed to foreign Ags but are not infected (31). Consequently, in general, exogenous Ags do not prime CTL responses in vivo. However, there are several exceptions to this rule, reflecting an ability of the Ags to be delivered into the cytosolic compartments (32–36). In the present study, Ags coupled to liposome consisting of unsaturated fatty acid were presented to both $CD4^+$ and $CD8^+$ T cells (Table I). Confocal laser scanning microscopic analysis demonstrated that a portion of the OVA coupled to liposomes received processing beyond the MHC class II compartment (Fig. 2), suggesting that degradation of OVA occurs in the cytosol and that peptides generated in this manner would be presented to $CD8^+$ T cells via MHC class I. Cross-presentation induced by OVA coupled to liposomes consisting of unsaturated fatty acids was further confirmed in the in vivo CTL induction experiments (Fig. 3). CTL were successfully induced in vivo only when OVA or $OVA_{257-264}$ chemically coupled to unsaturated liposomes were inoculated into mice. It is unlikely that the results were affected by contamination of the liposome preparation with endotoxin, since the liposomes used in the present study were produced using endotoxin-free materials in the GMP-verified production facilities of Nippon O.I. & Fats, which produces injection-grade liposomes for clinical use. In fact, SAC incubated for 2 h with OVA-liposome and subsequently cultured for 24 h did not produce any detectable cytokines, and the addition of polymixin B in the experiments shown in Table I did not affect the results (data not shown).

We next investigated the ability of Ag-liposome conjugates to induce antitumor immunity. The aim of cancer vaccination is to generate an immune-mediated antitumor-associated Ag (TAA) response resulting in the elimination of the tumor. The Ag of choice may be the whole protein alone or with immune stimulatory components, or defined epitopes (e.g., peptides) of the target Ag (7). Recent preclinical studies (37) have demonstrated that combined therapies involving the use of vaccines with cytokines, activators of DC such as TLR ligands or mAb to CD40, or recombinant vectors that provide a stimulus to the innate immune system resulted in enhanced antitumor responses. In the present study, antigenic peptides were chemically coupled to the surface of liposomes and inoculated into tumor-bearing mice in combination with CpG and anti-IL-10 mAbs. This treatment successfully induced eradication of the tumor mass, whereas inoculation of mice with CpG and anti-IL-10 mAbs with peptide solution containing the same amount of $OVA_{257-264}$ as liposome-coupled $OVA_{257-264}$ did not affect E.G7 tumor growth (Fig. 4). It has been reported that CpG and anti-IL-10 receptor Ab reverse tumor-induced DC paralysis, resulting in tumor rejection by CTL activated by the DC (38). However, under the conditions used in the present study, a combined inoculation of CpG and anti-IL-10 Abs in tumor-bearing mice did not inhibit the growth of the E.G7 tumor. In addition, the same Ag dose of plain peptide solution did not affect tumor growth even when inoculated in combination with CpG and anti-IL-10. Thus, liposome-coupled OVA peptide might be critical for the tumor eradication observed in the present study, suggesting that the administration of tumor Ag is indispensable for the induction of Ag-specific CTL, and peptide-liposome conjugates might effectively induce cross-presentation in APCs and induce a CTL response. In fact, tetramer staining (Fig. 4) demonstrated that Ag-specific CTL were significantly generated in mice that received